

# **Preparation and characterisation of nanocomposite thin films applicable in organic electronics**

Ing. Jakub Ševčík, Ph.D.

Doctoral Thesis Summary



**Tomas Bata University in Zlín**  
**Faculty of Technology**

Doctoral Thesis Summary

**Preparation and characterisation of nanocomposite  
thin films applicable in organic electronics**

**Příprava a charakterizace nanokompozitních tenkých filmů  
s využitím v organické elektronice**

Author: **Ing. Jakub Ševčík, Ph.D.**

Study Programme: P 2808 Chemistry and Materials Technology

Study Course: 2808V006 Technology of Macromolecular Compounds

Supervisor: Assoc. Prof. Ing. et Ing. Ivo Kuřitka, Ph.D. et Ph.D.

External examiners: Assoc. Prof. Dr. Ing. Vladimír Pavlínek  
Prof. Ing. Petr Slobodian, Ph.D.  
Prof. Ing. Mohamed Bakar, Ph.D.

Zlín, December 2019

© Jakub Ševčík

Published by **Tomas Bata University in Zlín** in the Edition **Doctoral Thesis Summary**.

The publication was issued in the year 2019

*Klíčová slova: Tenké vrstvy, nanokompozity, oxid zinečnatý, inženýring zakázaného pásu, PLED, konjugovaný polymer, MEH-PPV, organická elektronika, optoelektronické vlastnosti*

*Keywords: Thin-film, nanocomposite, zinc oxide, bandgap engineering, PLED, conjugated polymer, MEH-PPV, organic electronics, optoelectronic properties*

Full text of the scientific publication is available in the Library of TBU in Zlín.

ISBN 978-80-7454-890-1

## ACKNOWLEDGEMENT

I would like to express my sincere gratitude to my supervisor doc. Ing. et Ing. Ivo Kuřitka, Ph.D. et Ph.D. for his guidance, advices, and encouragement in my doctoral study.

Assistance in professional activities as well as personal help provided by my consultant Ing. Pavel Urbánek, Ph.D. was much appreciated.

I am particularly grateful to prof. Ing. František Schauer, DrSc., from the Faculty of applied informatics of the Tomas Bata University in Zlín, and to Dr. Vojtech Nádaždy from the Institute of Physics of the Slovak Academy of Sciences in Bratislava who founded the unique energy-resolved electrochemical impedance spectroscopy method and developed the first apparatus hitherto unavailable in any other laboratory. This original method was especially useful for the presented dissertation. Dr. Vojtech Nádaždy is also acknowledged for granting access to the apparatus in the laboratory of the Institute of Physics.

I wish to acknowledge the help with surface photovoltage method, conductivity measurements, and other experimental thin film characterisation methods provided by doc. RNDr. Jana Toušková, CSc., and RNDr. Jiří Toušek, CSc., from the Department of Macromolecular Physics, Faculty of mathematics and physics, Charles University. Their support during my stay in Prague, as well as the discussions of obtained results, are greatly acknowledged.

Dr hab. inż. Iwona Zarzyka provided me with very valuable experience of the Erasmus stay at the University of Technology in Rzeszów, Poland.

My colleagues and friends are deeply acknowledged for fruitful discussions and always positive attitude. Among them, specifically bits of advice given by Mgr. David Škoda, Ph.D., has been a great help in work with nanoparticle dispersions and thin-film nanocomposites. Thaiskang Jamatia, MSc., is acknowledged for the preparation and synthesis of most of the nanoparticles used in this work. My thanks are also extended to Ing. Jan Antoš, Ph.D., for the development of I-V measurement techniques and software used in our laboratories.

Special thanks belong to my family and friend for all their love, support, and encouragement throughout my studies.

I also acknowledge support and facilities provided by the Centre of Polymer Systems and the Faculty of technology of the Tomas Bata University in Zlín.

The internal grant agency of the TBU in Zlín provided funding of the Research in the projects No. IGA/CPS/2015/006, IGA/CPS/2016/007, IGA/CPS/2017/008, IGA/CPS/2018/007, and IGA/CPS/2019/007.

The Ministry of Education, Youth and Sports of the Czech Republic is acknowledged for support within the National project of sustainability NPU I LO1504 – Centre of Polymer Systems plus.

The Czech Science Foundation (GA CR) is acknowledged for financing the project GA19-23513S.

Finally, the Technology Agency of the Czech Republic (TA CR) supported the project TE01020216.

All specific financial support granted to my work is also acknowledged in the respective places in my published articles, submitted manuscript or prepared papers.

# CONTENT

Abstract .....	2
Abstrakt .....	3
1. Introduction.....	4
1.1 Organic and Polymer light-emitting diode (OLED and PLED) .....	4
1.2 The density of states (DOS) .....	5
2. Thin film preparation techniques in PLEDs .....	7
3. Aim of Doctoral thesis.....	8
4. Experimental section.....	9
4.1 Chemicals and materials.....	9
4.2 Samples preparation .....	9
4.3 Characterisation techniques.....	11
5. Results and discussions.....	13
5.1 Surface photovoltage of thin polymer films.....	13
5.2 Neat MEH-PPV diodes .....	16
5.3 Nanocomposite diodes .....	17
5.4 Performance of prepared devices .....	26
6. Conclusions.....	31
7. Closing remark.....	34
7.1 Contribution to science and practice .....	34
7.2 Ongoing research and future prospective.....	35
References .....	35
List of Tables.....	39
List of Figures .....	40
List of abbreviations and acronyms .....	41
List of symbols.....	42
Curriculum Vitae.....	44
List of projects.....	45
List of publications.....	45
Overview of other activities.....	47

## ABSTRACT

In this work, the recently obtained experimental results in the field of bandgap engineered nano ZnO/MEH-PPV (poly[2-methoxy-5-(2-ethylhexyloxy)-1,4-phenylenevinylene]) are presented, mainly thin nanocomposite films preparation, their electronic structure and properties characterization and implementation of them as active layers into the PLED devices. The influence of the nanoparticle size and composition, the thickness of thin films and parameters during their preparation on the optoelectronic properties and PLEDs performance are studied. Electronic structure of such nanocomposite films was studied with energy-resolved electrochemical impedance spectroscopy for the first time. Addition of any of the studied nanoparticles enhanced the luminance of prepared diodes in comparison with reference samples made from neat MEH-PPV polymers. Nanoparticle concentration, size and thin film thickness optimum was found for pure ZnO system within the range of tested parameters. Two principally different dopants – iron and aluminium – were used to modify the bandgap of the material and effects of concentration of the dopants in nanoparticles was investigated. The Fe-doping decreases the maximum luminance of the diode at given operating voltage in comparison with the reference undoped ZnO nanocomposite; however, it also decreases the opening bias significantly. Thus, Fe-doping opens a way to a search for the best balance between these two effects and finding an optimum power efficiency in this case. Significant enhancement of examined performance parameters in comparison with the reference undoped ZnO system was achieved for Al-doped samples. Both the opening bias and luminance of the diode were greatly enhanced by using this material.

**Keywords:** Thin-film, nanocomposite, zinc oxide, bandgap engineering, PLED, conjugated polymer, MEH-PPV, organic electronics, optoelectronic properties

## ABSTRAKT

V této práci jsou prezentovány nedávno dosažené výsledky v oblasti optimalizace band-gapu na nanokompozitních materiálech ZnO/MEH-PPV (poly[2-methoxy-5-(2-ethylhexyloxy)-1,4-phenylenevinylene]), především pak příprava tenkých nanokompozitních filmů, charakterizace jejich elektronové struktury a elektronických vlastností a jejich implementace jako aktivní vrstvy do PLED zařízení. Velikost částic a jejich atomární složení, tloušťka vrstev a parametry přípravy těchto vrstev byly studovány vzhledem k jejich vlivu na výsledné optoelektronické vlastnosti a výkon PLED zařízení. Elektronová struktura takových nanokompozitních vrstev byla vůbec poprvé studována pomocí energeticky rozlišené elektrochemické impedanční spektroskopie. Bylo objeveno, že přídavek kterýchkoliv ze studovaných nanočástic významně vylepšuje svítivost připravených diod ve srovnání s diodami z čistého polymeru. Byla nalezena optimální koncentrace nanočástic, jejich velikost a optimální tloušťka nanokompozitního filmu, nejdříve pro systém s čistým ZnO. Dále pak bylo provedeno dopování nanočástic různými dopanty – železem a hliníkem, což mělo za následek modifikaci stavové struktury v band-gapu. Dopování nanočástic železem snižuje svítivost nanokompozitní emisní vrstvy ve srovnání s použitím čistých ZnO nanočástic, nicméně také se významně snižuje otevírací napětí diod. A proto dopování nanočástic pomocí Fe otevírá cestu, jak co nejlépe balancovat vliv těchto dvou efektů, a jak optimalizovat energetickou účinnost zařízení. Významného zlepšení u výkonu PLED zařízení bylo dosaženo použitím Al dopovaných nanočástic oproti nanočásticím z čistého ZnO. Jak otevírací napětí, tak i svítivost, byly významně vyšší s použitím Al dopovaných nanočástic.

**Klíčová slova:** Tenké vrstvy, nanokompozity, oxid zinečnatý, inženýring zakázaného pásu, PLED, konjugovaný polymer, MEH-PPV, organická elektronika, optoelektronické vlastnosti

# 1. INTRODUCTION

## 1.1 Organic and Polymer light-emitting diode (OLED and PLED)

Organic light-emitting diodes (OLEDs) represent a type of devices using organic semiconductors as the emissive electroluminescent layer to emit light in response to an external electric current. The OLEDs have a multi-layered structure composed of an organic semiconductor inserted between two electrodes of which at least one must be transparent. The working principle of OLEDs is similar to the LEDs, but instead of using n-type and p-type semiconductors, they utilise organic molecules to produce their electrons and holes. OLEDs are managed under the external voltage that is applied on the electrodes, through which the electrons and holes are driven to the recombination centres within the emission layer. These leads to the recombination of charge carriers (they are bounded together by Coulomb forces) which generates quasi-states of electron-hole pairs called excitons. Related to the lifetime of excitons, the energy is then released from the Coulomb interaction in the form of photons whose wavelength depends on the width of the band-gap of semiconducting materials forming the active layer. Typically, to improve the charge transport efficiency from the electrode to the electroluminescent sites, a segment of the electron transporting layer and hole transporting layer can be incorporated into the OLED layered structure as shown in Figure 1.

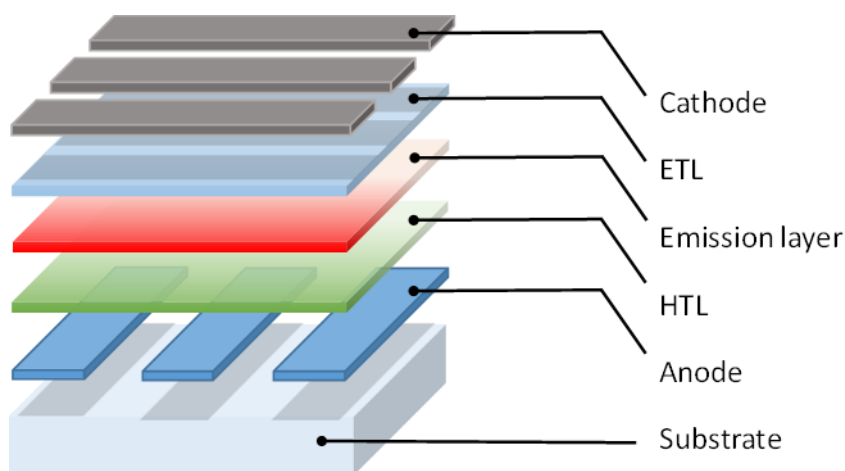


*Figure 1. The schematic representation of a simple OLED device structure*

There are two basic approaches related to OLEDs: small-molecules (SM-OLED) or large-molecules, respectively polymers (PLEDs). The majority of OLED displays on the market today are applying Small Molecules, and are produced using by costly evaporation processes. Various kinds of polymers have been identified as a promising class of materials for optoelectronic applications

like light-emitting devices. A polymer that can be used as light-emitting material must have two fundamental characteristics- electrical conductivity and high photoluminescence efficiency. Conjugated polymers (CPs) are the typical representatives of conductive polymers and can be classified as organic macromolecules that are characteristic by backbone chain of alternating double- and single- bonds. According to the band theory in semiconductors, the luminescence produced by the light-emitting polymer (LEP) as a response for an external initiative has the energy (wavelength) related to the energetic width of the bandgap. The next advantage of CPs lies in the virtually infinite possibilities for creating new materials or composites for specific applications by chemical or physical tuning of the molecular structure. Physical modification can be interpreted as the incorporation of nanoparticles of different nature and size into the conjugated polymer matrix.

The idea of using of nanocomposites in the field of organic electronics is based on band-gap adjusting and charge carriers balancing according to equation 1.

$$\eta_{EQE} = \gamma \times \eta_{S/T} \times q_{eff} \times \eta_{out} \quad (1)$$

where  $\gamma$  is a factor expressing whether are the charges in equilibrium;  $\eta_{S/T}$  is the ratio of singlet and triplet excitons;  $q_{eff}$  is a factor representing the efficiency of excitons contributes to radiative recombination;  $\eta_{out}$  indicates the number of irradiative photons [1-3].

## 1.2 The density of states (DOS)

As mentioned several times above, the density of states is another fundamental characteristic in the field of electronics, which plays a crucial role in charge transport phenomena. The density of states function specifies the number of states at a particular energy level that is available in a system for occupation by electrons, i.e. the number of electron states per unit volume per unit energy.

### 1.2.1 Measurement of DOS by Electrochemical impedance spectroscopy (ER-EIS)

The method is based on measuring the charge transfer resistance at the semiconductor/electrolyte interface at a frequency where redox reactions define the real component of the impedance. The charge transfer resistance value

represents direct information about the electronic DOS at the energy given by the electrochemical potential of the electrolyte, which can be modified by an external voltage. A simple theory for experimental data estimation is suggested, along with a clarification of the appropriate experimental conditions. The approach allows mapping over abnormal wide energy and density of states ranges. Important DOS parameters can also be determined directly from raw experimental data without the unnecessarily time-consuming analysis required in other techniques [4]. The semiconductor/electrolyte interaction is similar to

the extraction and capture of an electron by an acceptor and donor on a semiconductor surface through the medium of conventional solid-state reactions. The charge-transfer current density  $j$  between the semiconductor surface with a concentration of electrons  $n_s$  and electrolyte with concentration  $[A]$  of redox (donor/acceptor) pair is:

$$j = ek_{et}n_s[A] \quad (7)$$

, where  $e$  is the elemental charge and  $k_{et}$  is the coefficient of charge-transfer in the  $10^{-17}$ – $10^{-16}$   $\text{cm}^4 \text{s}^{-1}$  range. The electron concentration on semiconductor surface  $n_s$  is a variable that can be characterised and controlled experimentally by selecting the semiconductor surface potential. When the concentration of states on the surface of the organic film is insignificant, then data about the electron allowed states of the organic film at the energy level corresponding to the immediate electrochemical electrolyte potential can be acquired directly. Various elementary semiconductor/electrolyte processes respond to system failures at different speeds, and the corresponding relaxation processes become dominant in the impedance spectra measured at different frequencies  $\omega$ .

Hence, the individual components of these processes can be identified and distinguished by measuring impedance over a certain frequency range. Using Equation 7, the DOS function in the semiconductor at the Fermi energy  $g(E_F)$  can be expressed in terms of the charge transfer resistance  $R_{ct}(U)$  measured under applied voltage  $U$  as:

$$g(E_F = eU) = \frac{dn_s}{d(eU)} = \frac{1}{ek_{et}[A]S} \frac{d(jS)}{d(U)} = \frac{1}{ek_{et}[A]SR_{ct}} \quad (8)$$

The measurements were carried out using a conventional three-electrode electrochemical cell system with a volume of approx — 200  $\mu\text{l}$ . The polymer film spin-coated on the indium tin oxide (ITO) substrate represented the working electrode, while the Ag/AgCl and Pt wires were the reference and auxiliary electrodes, respectively. This setup is illustrated in

Figure 2.

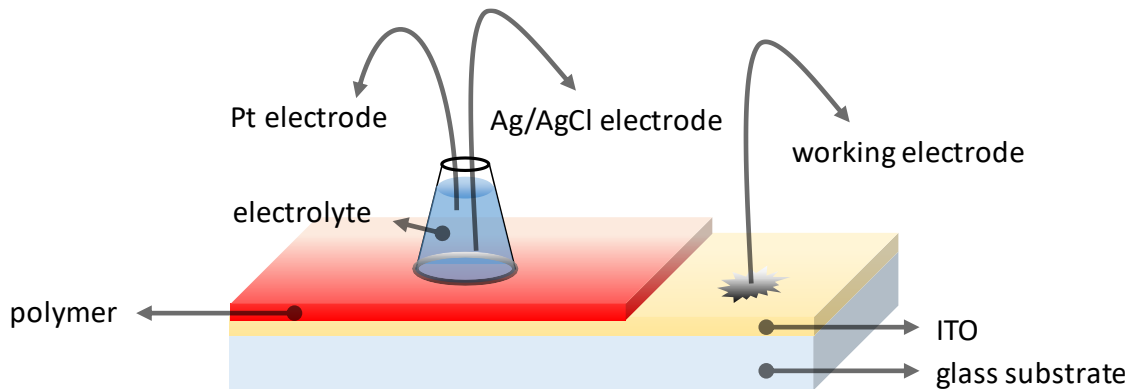


Figure 2 Sample arrangement of ER-EIS method

## 2. THIN FILM PREPARATION TECHNIQUES IN PLEDS

Methods of thin films deposition may be divided mainly into two main categories, namely chemical methods (including electrochemical methods) and physical methods. We shall focus primarily on physical processes because they result in the formation of very pristine and well-defined films. In operation, they are applicable to all materials and a considerable range of thicknesses. The choice of deposition technique and its implementation are one of the critical factors for preparing thin-film devices. While the conventional OLEDs are prepared mainly by costly vacuum-requiring deposition processes, the functional core of the PLEDs can be deposited from solution due to the solubility of components used [5, 6].

### 2.1.1 Spin coating

Spin coating is a relatively cheap, swift and reproducible technique for depositing of thin, homogeneous layers from a solution. It is widely used in microelectronics, for example in the production of photoresists.

The process can be divided into several steps. Firstly, the substrate is placed on the rotor seal ring and immobilised by a vacuum pump. The rotor accelerates in the next step to the required rotation speed, during which the polymer solution is dripped on the substrate and formed by the centrifugal forces from the centre to the edges. Part of the solvent is directly removed and the residual will evaporate by heating above evaporation temperature  $T_v$  [7].

In the case of time-independent non-Newtonian solutions, the thickness of the resulting layer can be predicted according to the following model:

$$\delta = K.c.\left(\frac{\nu}{\omega^2 + R^2}\right)^{1/3} \quad (18)$$

where  $\nu$  is the kinematic viscosity,  $c$  is the volume fraction of solids,  $\omega$  is the angular velocity;  $R$  is the disk radius or average symmetrical dimension of the sample;  $\delta$  is the dry coating thickness;  $Q$  is the volumetric flow rate; and  $K$  is a constant  $(81Q/16 \pi)$  [8].

### 3. AIM OF DOCTORAL THESIS

The aim of the work is the development of material systems for enhancement of performance of PLEDs based on MEH-PPV polymer and doped ZnO nanoparticles with particular focus on the luminance intensity, lowering of bias voltage (turn-on voltage), and luminance efficiency.

The accomplishment of the aim may be outlined in the following goals and objectives:

- Standard, neat polymer diode preparation.
  - In order to fulfil this goal of the study, neat polymer LEDs needs to be prepared as reference samples with standard performance. The p-type polymer MEH-PPV will be used as the most studied model polymer.
  - This requires optimisation of the PLED fabrication process in actual conditions and with the use of equipment available in our workplace. Thus, ITO pre-fabricated substrates need to be used. All supporting and active layers will be deposited by a wet process, including optimisation of PEDOT:PSS HTL preparation. Top electrodes can be sputtered from non-oxidizing metals (gold, silver, aluminium or magnesium). The key steps work will be performed in a glove box with a nitrogen protective atmosphere enabling final encapsulation of prepared device into transparent resin. Proper cleaning and surface preparation techniques shall be used throughout the work.
  
- Study of effects of doped ZnO nanoparticles incorporation into polymer active layer of prepared devices.
  - ZnO nanoparticle dispersions with pure ZnO or doped ZnO will be mixed with polymer solution in order to prepare PLEDs comparable with neat polymer standards. All other conditions will be kept the same (*ceteris paribus*). Performance of prepared diodes will be studied and obtained results interpreted. Received feedback will be used throughout the experimental work to improve prepared devices.
  - According to the literature review, the concentration of positive and negative charge carriers should be balanced to achieve maximum theoretical efficiency. Therefore, n-doping of ZnO will be preferably utilised. Moreover, the effects of the nanoparticle bandgap modification onto the electronic structure of the active nanocomposite layer and characteristics of the devices (opening voltage, I-V(-L) curves) will be studied, and their influence on the device performance analysed.
  
- Morphology and electrical measurements methods for characterisation of prepared devices will be applied.

- AFM and optical profilometry of thin polymer and nanocomposite film and eventually SEM will be used.
- The thickness of the prepared layer will be characterised with the aid of mechanical and optical profilometers and by the spectroscopic ellipsometry.
- Improvement of in-house available electrical characterisation techniques is expected. The utilisation of techniques available at the Institute of Physics of the Slovak Academy of Sciences (energy-resolved EIS) and Department of Macromolecular Physics at the Faculty of Mathematics and Physics (SPV, impedance spectroscopy, conductivity measurements) is expected.

## 4. EXPERIMENTAL SECTION

The experimental part of this thesis will be related to the preparation of the multi-layered PLED device, which will be organized to these separate segments:

### 4.1 Chemicals and materials

#### *Commercial chemicals and materials*

Toluene (p.a.), and methanol (p.a.) were purchased from PENTA Czech Republic. MEH-PPV Poly [2-methoxy-5-(2-ethylhexyloxy)-1,4-phenylenevinylene] ( $M_w = 40000\text{--}70000\text{ g mol}^{-1}$ ) was purchased from Sigma-Aldrich. PEDOT:PSS (poly (3,4-ethylenedioxythiophene)polystyrene sulfonate) was supplied by Heraeus (Clevios™ P AI 4083). Commercial ZnO nano-powder, particle size < 50 nm (TEM) purchased from Sigma-Aldrich.

#### *Synthesised chemicals and materials*

Neat ZnO nanoparticles without dopants, Fe-doped and Al-doped ZnO nanoparticles  $\text{Fe}_x\text{Zn}_{1-x}\text{O}$  and  $\text{Al}_x\text{Zn}_{1-x}\text{O}$  ( $x = 0,01; 0,05; 0,10$ ) were synthesized in our workplace. The synthesis protocols particles were published elsewhere and are out of the scope of this thesis.

### 4.2 Samples preparation

#### 4.2.1 Solutions/dispersions preparation

A variety of polymer solutions has been prepared to understand the behaviour of used polymeric materials. Particular attention was paid to the solution concentration. On the other hand, many operations such as solvent purification, the time and intensity of the mixing process or method of storage were applied equally regardless of the type of material being prepared. For the preparation of dispersions of nanoparticles in the polymer solution, the 20 minutes of sonication in the ultrasonic bath was added to the process.

The neat solvents were filtered by the 0,45  $\mu\text{m}$  PTFE syringe filters just before every use. All prepared polymer solutions were stirred overnight (approx. 12 h) under 120 revolutions per minute and kept in the fridge. With regard to the volatility of the solvents used, these materials were applied as soon as possible to the next step of preparation of thin films. All of these operations were performed in ambient temperature at atmospheric pressure. The two following types of solutions or dispersions were prepared:

#### *MEH-PPV solutions*

In the preparation of MEH-PPV solutions, these variety concentrations of polymer in toluene were used (2,9 mg/ml; 5 mg/ml; 10 mg/ml; 20mg/ml).

#### *(MEH-PPV)/nanoparticles dispersions*

For the purposes of polymer/inorganic nano-dispersions preparation, the dispersions with 10 mg of nanoparticles in 3,5 ml of toluene were synthesized by other members of our group and used after thoroughly performed characterization. In a standard case, 10 mg of conjugated polymer (MEH-PPV) were added to the dispersion to keep the weight ratio polymer/nanoparticles 1:1. The ratio was kept the same for all, but one study. In the study with commercial ZnO nanoparticles, it varied from 4:1 to 1:1 in nanocomposites used as the active layer in PLEDs. Taking the density of MEH-PPV (0.98 g/cm<sup>3</sup>) and density of ZnO (5.61 g/cm<sup>3</sup>), the volume percentage of the filler in the thin film varied from ca 5 to 15 vol%.

### **4.2.2 Thin-film preparation**

With respect to the requirements of excellent adhesion and absence of impurities, substrates were chemically cleaned and etched in an ultrasonic bath and immediately before deposition the final surface modification by the ozone cleaner was carried out. The prepared mixtures (solutions or dispersions) were used as a precursor for thin-film preparations in a nitrogen atmosphere in a glove box. Thin films were prepared by spin coating the solution on three types of substrates (ITO-coated glass, quartz glass and silicon wafers) at a variety of rotational speed for 30 s. The samples were then kept for drying on a hot plate at 150 °C for 30 minutes. Prepared samples were left to cool naturally and transferred out from the glovebox. The topography and thicknesses of produced thin films were characterised as well as the optoelectronic properties.

### **4.2.3 PLED fabrication**

Polymer light-emitting devices were fabricated as follows. The PLED devices with a neat polymer as an active layer consisted of MEH-PPV or F8BT were prepared in an inert (N<sub>2</sub>) atmosphere as follows: Standardly patterned (Ossila Ltd.) ITO substrates with six active pixels were used for device fabrication. PEDOT:PSS was filtered through a 0,45  $\mu\text{m}$  PVDF filter prior to being deposited as HTL (hole - transporting layer) by standard procedure. The solution of MEH-

PPV in toluene (100  $\mu$ l) was spin-coated onto the HTL layer to get the desired thickness, followed by drying at 150  $^{\circ}$ C on a hot plate. Then, a magnesium cathode was sputtered by Quorum Technologies Q300TT sputter-coater. For the study of PLEDS with polymer blends, mixed solutions were used for casting of the active layer. In the case of nanocomposite based PLEDs, the same procedure was used but the solution of a neat polymer was replaced by the dispersion of nanoparticles in the polymer solution. The scheme of fabrication and the structure of a PLED device are displayed in Figure 3. All PLED devices were encapsulated by an epoxy resin before removing them from the protective atmosphere.

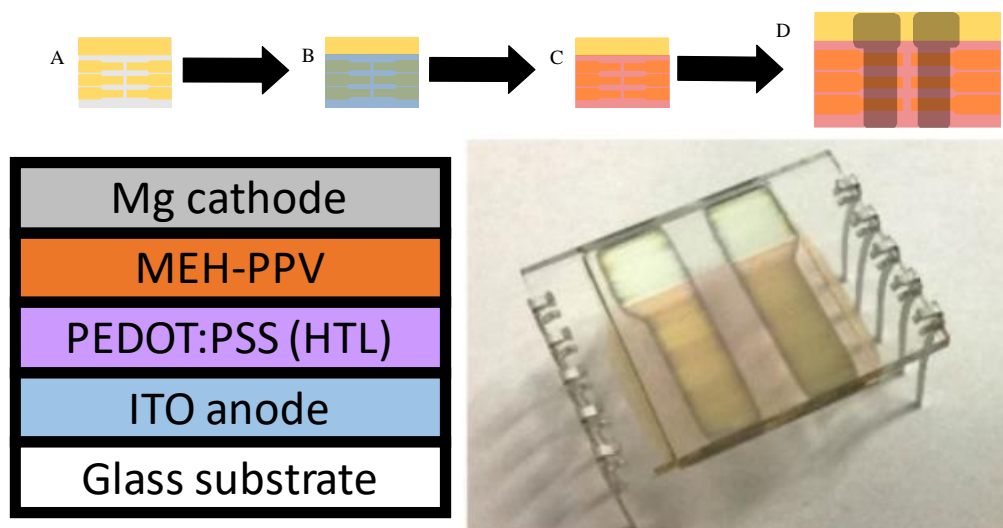


Figure 3 Scheme of fabrication of PLED; a) glass with patterned ITO, b) deposition of HTL PEDOT:PSS, c) Deposition of active layer; d) Sputtering of metal Cathode

### 4.3 Characterisation techniques

Morphologies on the cross-section of devices were investigated by a NovaNanoSEM 450 scanning electron microscope (The Netherlands, FEI Company) with Schottky field emission electron source operated at acceleration voltage ranging from 200 V to 30 kV.

The elemental microanalysis was performed by the Octane SSD (area 30 mm<sup>2</sup>) EDX (energy dispersive X-ray) detector (AMETEC, Inc).

The crystallinity and phase identification of powder materials were confirmed by XRD diffractometer MiniFlex600 (Japan, RIGAKU) with Co K $\alpha$  source. The size of the ZnO nanocrystallites was considered to the size of the diffracting area differ which is accessible via Scherrer's formula using  $\Delta(2\theta)$  which is full-width at half-maximum (FWHM) of the line in the XRD patterns.

The study of UV-vis diffuse reflectance of prepared powders was performed by the UV-vis spectrometer AvaSpec 2048-2 (Avantes, The Netherlands) with the light source AvaLight-DHS-DUV equipped with an integrating sphere (BaSO<sub>4</sub> coated) and white tile BaSO<sub>4</sub> reflectance standard.

The study of the UV-vis absorption of the solutions was performed with the aid of the UV-vis spectrometer UV-Vis Varian Cary 300 (Varian Inc., United States).

The PL spectra were taken in a vacuum (pressure 1 Pa) ensured by the cryostat Optistat DN-V (LN<sub>2</sub>), Oxford Instruments at room temperature.

The thickness of films, measured by a mechanical profilometer Dektak XT-E and (Bruker) with a 1 nm resolution and optical profilometer CONTOUR GT-K images surfaces and roughness in 2D/3D based on phase-shifting interferometry (PSI mode) and vertical scanning interferometry (VSI mode). Maximal scan range is 10 mm, vertical resolution < 0.01 nm (as indicated by Bruker) and lateral resolution < 0.5 μm. The topography of thin films, measured by atomic force microscope Dimension ICON (Bruker). The microscope allows nanoindentation measurement with a diamond pin.

The transmission electron microscopy was carried out on a TEM JEOL JEM 2100 operated at 300 kV (LaB<sub>6</sub> cathode, point resolution 2.3 Å equipped with OLYMPUS SYS TENGRA camera (2048 x 2048 pixels). The particle size distributions were calculated with the use of OLYMPUS Soft Imaging Solutions software. The TEM samples were prepared by dropping the colloid sample solution on carbon-coated copper grids (300 mesh) and drying at 80 °C (1 h).

The thin films were deposited on an ITO patterned glass substrate by a spin coating method using the spin coater Laurell WS-650-MZ-23NPP.

The electroluminescence spectra and luminance measurements were collected on a UV/Vis spectrometer Avantes Avaspec 2048 using an integration sphere with 50 mm diameter. A comparison with a diode B5-433-20 (Roithner Laser-technik, Ltd., Austria) of known luminance was used for estimation of the luminance of prepared devices.

The current/voltage characteristics were obtained by a multimeter HP 34401A and a power supply system HP 6038A in conjunction with using “C/V Charakteristika 2.1” software developed at our institute by Jan Antoš in Labview.

Variable-angle spectroscopic ellipsometry UVISEL 2 (Horiba) with a spectral range from 180 nm to 2200 nm and a resolution higher than 0.5 nm was used to determine optical constants and changes in polarization angles and their wavelength dependence. The data was then used to calculate the film thickness using Delta Psi V2 software.

To determine the diffusion length of excitons of prepared thin polymer films, the surface photovoltage method was used. This machine was constructed by colleagues from Charles University. It consists of a source of light, beam splitter, monochromator, amplifier and voltmeter.

The novel spectroscopic method, Energy-resolved electrochemical impedance spectroscopy (ER-EIS), is used for the measurement of the density of states (DOS). The ER-EIS method is based on the analysis of the charge transfer resistance,  $R_{ct}$ , of a semiconductor/electrolyte interface at a frequency where the redox reactions determine the real component of the impedance.

## 5. RESULTS AND DISCUSSIONS

The main focus of the work is laid on experimental preparation and characterisation of PLEDs. A large number of results have been achieved in directions outlined by the goals of work. Namely, the work on thin polymer and nanocomposite films, standard and nanocomposite MEH-PPV based PLEDs preparation and characterisation is highly advanced. This chapter summarises the experimental results achieved in detail, in which the material and thin films characterisation are followed by PLED devices characterisation. Moreover, the results are discussed along their presentation, so the reader does not lose context.

### 5.1 Surface photovoltage of thin polymer films

The conformational order and in  $\pi$ -conjugated polymer stacks must influence the diffusion length of the exciton. Therefore, the SPV method can be used with advantage to determine this behaviour because it is independent of the film thickness. So, it is sensitive to the changes of diffusion length varying with thickness. To confirm and reinvestigate these results, additional and repeated measurements were performed. A typical obtained result of SPV characterisation is illustrated in Figure . An example of an experimentally recorded SPV spectrum for the MEH-PPV thin film with the thickness 60 nm (open circles) and the theoretical curve fit (solid line) into the data are plotted in the figure. Note the similarity of the SPV signal to the UV-Vis absorption spectrum of the material (for comparison see elsewhere [9]). The diffusion lengths were evaluated using the theory included in part of theoretical chapter 2.7.

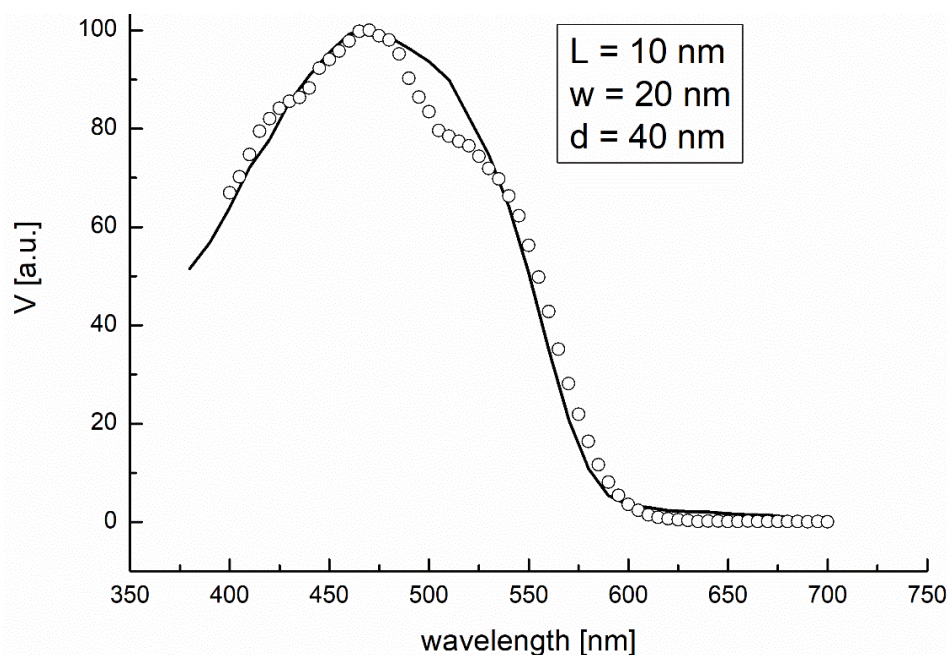


Figure 4 A representative of the SPV measurement and evaluation of diffusion length of excitons. Own source.

Reflectance measured for all individual thicknesses and absorption coefficients were used for the theoretical spectra calculation. The diffusion lengths of excitons were obtained by fitting the theoretical SPV spectra (full lines) to the experiment (points). The mathematical fit is in good accordance with the measured spectra in all cases. The obtained values of the exciton diffusion length are listed in Table 1. The hypothesis of threshold thickness for optoelectrical properties implying non-trivial polymer film structure dependence on the film thickness [9] was confirmed. According to that, one may suggest that the thickness of the active layer should be tested either below or above the threshold limit to see eventually clear trends.

*Table 1 Highlighted diffusion lengths of excitons and their dependency on film thickness. The values without reference are newly obtained.*

<b>The thickness of the MEH-PPV film</b>	<b>Diffusion length of exciton</b>
19 nm	15 nm [9]
53 nm	9 nm [9], 7 nm
60 nm	15 nm
85 nm	18 nm [9], 20 nm
100 nm	16 nm
200 nm	36 nm
235 nm	43 nm [9], 40 nm
310 nm	65 nm [9], 75 nm

### 5.1.1 Photoluminescence of thin nanocomposite films

Figure 4 represents the room temperature PL spectra of pure MEH-PPV, ZnO/MEH-PPV, Fe<sub>x</sub>Zn<sub>1-x</sub>O/MEH-PPV and Al<sub>x</sub>Zn<sub>1-x</sub>O/MEH-PPV composite films with different Fe concentrations ( $x = 0, 0.01, 0.05, 0.10$ ) and Al concentration ( $x = 0.01, 0.05, 0.10$ ) at excitation wavelength 515 nm. To remind, the concentration of particles was 50 wt%, i.e. 15 vol% in prepared films. The wavelength range of emission from 560 nm to 800 nm is mainly due to the conductive polymer MEH-PPV. The incorporation of nanoparticles influences the intensity ratio of the 0-0/0-1 emission, which testifies to structural changes in the cast nanocomposite thin film.

Moreover, the peak around 590 nm and shoulder peak around 640 nm is attributed to the 0-0 and 0-1 vibronic transitions, respectively, due to excitonic recombination. An overall decrease in the PL intensity of the nanocomposite layers is assigned to polymer luminescence quenching caused by incorporating the nanoparticles into MEH-PPV. The reason for this quenching can be attributed to the photoinduced electron transfer from the LUMO of MEH-PPV to the conduction band of the ZnO semiconductor.

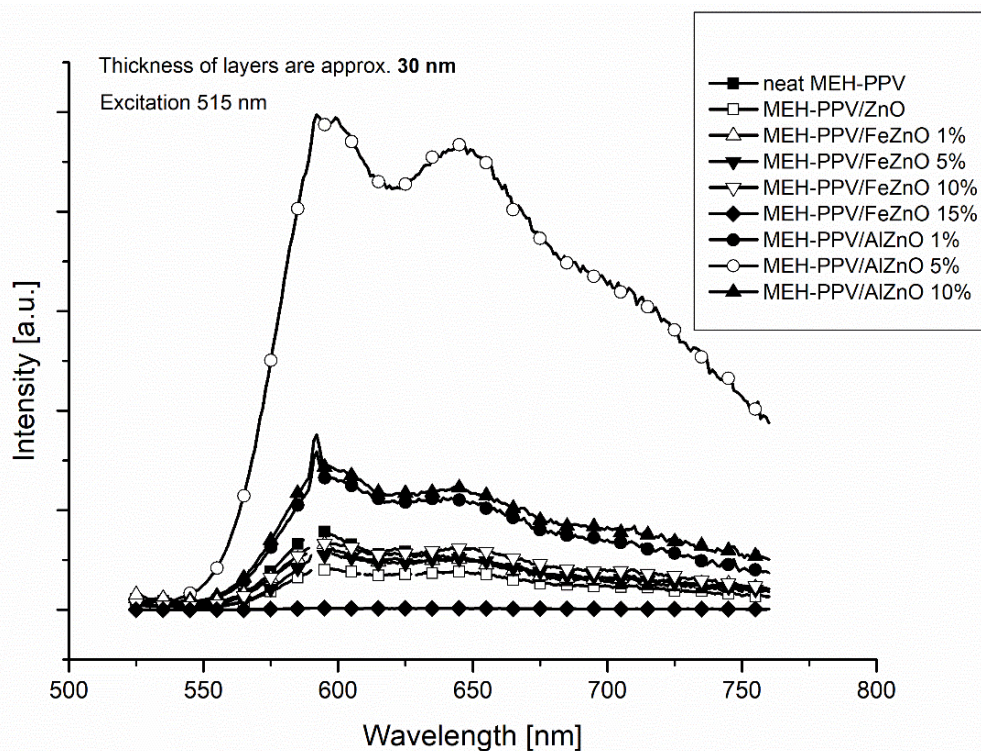


Figure 4 Emission scans of prepared thin nanocomposite films based on MEH-PPV conjugated polymer

### 5.1.2 Density of states of thin polymer and nanocomposite films

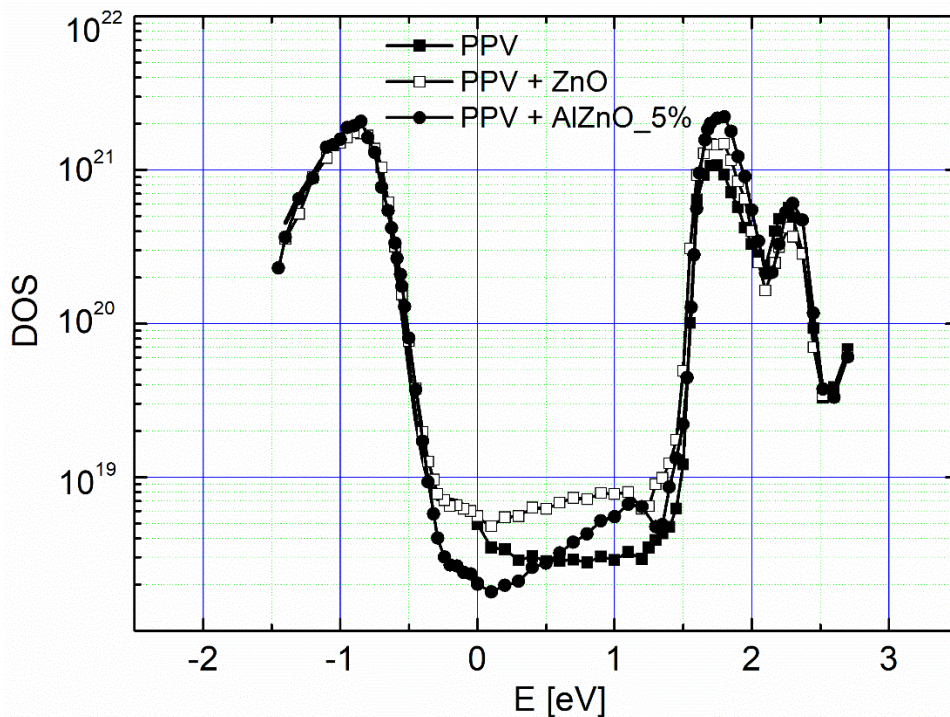


Figure 5. The density of states of MEH-PPV, MEH-PPV/ZnO and MEH-PPV/AlZnO layers with thickness approx. 100 nm

The electronic structure in terms of density of states function,  $g(E)$ , was measured in three conjugated polymer MEH-PPV based thin layers, including the deep states, which are crucial for recombination, and the shallow HOMO (highest occupied molecular orbital) and LUMO (lowest unoccupied molecular orbital) states, which are essential for charge transport. The energy scale is not recalculated from the applied bias voltage to the absolute energy scale using zero vacuum level. So, the zero on the energy scale corresponds to -4.66 V, which is the potential of silver chloride (Ag/AgCl) reference electrode. This DOS spectrum implies hopping charge transport via the Gaussian distributed localized states to be the predominant transport path. It can be clearly seen, that incorporation of nanoparticles into the polymer matrix influenced the density of states in the bandgap in comparison with neat MEH-PPV. In the case of nanocomposite prepared by incorporation of ZnO into MEH-PPV, the density of states is roughly one order of magnitude higher than neat MEH-PPV. This increase is observed over the whole width of the bandgap. It can be interpreted as a general increase of structural disorder in the polymer matrix which should result in a decrease of luminescence intensity. Indeed, the decrease of luminescence efficiency was observed for neat ZnO/MEH-PPV nanocomposite thin films. However, it can also be a manifestation of a specific doping effect of the nanosized n-semiconductor. This second explanation is confirmed by the increase in the electroluminescence intensity of the prepared light-emitting devices. In case of Al-doped nano ZnO, an even more pronounced effect can be seen. Aluminium is a negative dopant for ZnO. The increase of density of states nearby LUMO is due to the increase of the n-doping character of the nanoparticles with respect to the MEH-PPV polymer. Moreover, the density of deep states near HOMO of the polymer is decreased even in comparison with the neat MEH-PPV film. Explanation of this phenomenon due to filling of the traps is more likely than a (highly improbable) increase of conformational order of the polymer chains due to presence of nanoparticles. The first one of the two explanations is supported by observed increase of luminescence intensity from the Al-doped ZnO/MEH-PPV thin films.

## **5.2 Neat MEH-PPV diodes**

### **5.2.1 Characterization of PLEDs**

In order to grasp the studied problem systematically, standard PLEDs using MEH-PPV were prepared first. A series of preparational protocols and work procedures were developed for being applied in specific conditions in our workplace to assure serial coherence and repeatability of our results and their reproducibility or comparability with results obtained by other laboratories. At given material composition and PLED structure design, the thickness of the active layer is a primary parameter influencing the performance of the device.

Therefore, a study of the influence of MEH-PPV active layer thickness on current-voltage characteristics and intensity of electroluminescence was performed [10].

As summarised in Table 2, the opening voltage of the electrode depends linearly on the thickness of the active layer, which can be explained by the influence of serial resistance of the material or in other words by the need of constant electric field intensity for opening the diode. The maximum electroluminescence emission intensity decreases hyperbolically with the increasing thickness of the active layer, as one can intuitively expect since the diodes were forward-biased always by 10 V and the current depends inversely on the resistance of the sheet. Emission spectra have a typical shape for MEH-PPV photoluminescence spectra with prevailing radiative deexcitation between 0-0 vibronic levels corresponding to the emission peak maximum at the wavelengths below 600 nm, while the system 0-1 contributes by one third or less to the total electroluminescence intensity.

*Table 2 Highlighted parameters of PLEDs with neat MEH-PPV as an active layer*

<b>The thickness of MEH-PPV [nm]</b>	<b>opening bias [V]</b>	<b>EL intensity maximum powered by 10 V [arb.u.]</b>
30	6.1	11 800
45	5.5	14 360
80	10.1	4 600
100	11.1	2 300
150	14.0	460

### **5.3 Nanocomposite diodes**

The positive effect of ZnO as an n-type semiconductor in the design of PLEDs was already known. A separate layer of ZnO nanoparticles was previously used to improve electron injection from the cathode into the active layer. Unlike in the literature, we propose that it should be possible to mix n-type ZnO nanoparticles into the p-type conjugated polymer (MEH-PPV) matrix directly and enhance thus the efficiency of the PLEDs due to the improvement of the charge carrier balance.

#### **5.3.1 Nanocomposite diodes with undoped ZnO particles $\leq 50$ nm**

In order to verify the concept of nanocomposite active layer in PLED, commercially available ZnO nanoparticles were used. However, relatively thick polymer layers were cast due to the size of nanoparticles in range  $\leq 50$  nm. The images are not included for the sake of brevity. The average thickness of the active layer in prepared PLED samples was ca 150 nm. A study of the influence

of concentration of the nanoparticles incorporated into polymer matrix on I-V characteristics and intensity of EL was performed. The composition varied from 20 wt% up to 50 wt% of the filler in the nanocomposite, in other words, the weight ratio of the polymer to the particles varied from 4:1 up to 1:1; thus the volume percentage varied from ca 5 to 15 vol%. Obtained electroluminescence spectra are presented in Figure 6.

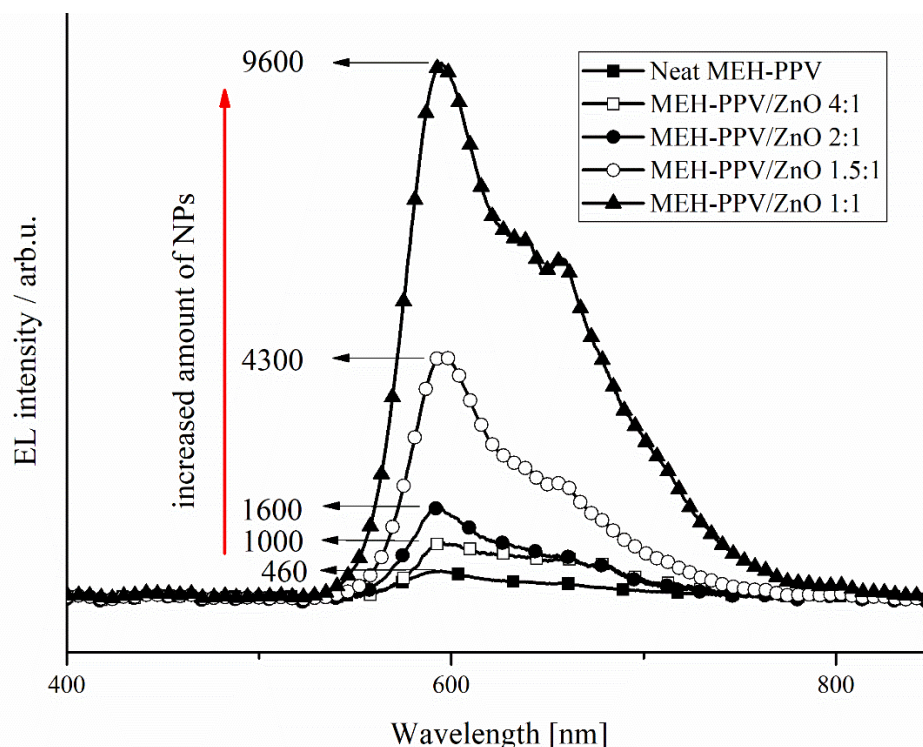


Figure 6 Intensity of electroluminescence of PLED devices MEH-PPV/ commercial ZnO as an active layer with input voltage 10 V and 1 s integration time

Table 3 Highlighted parameters of PLEDs with ZnO nanoparticles incorporated in 150 nm thick active layer with MEH-PPV matrix

the weight ratio of ZnO NPs in composite [wt%]	opening bias [V]	EL intensity maximum powered by 10 V [arb.u.]
0	13.6	460
20	9.8	1 000
33	8.7	1 600
40	6.7	4 300
50	6.5	9 600

Table 3 summarises essential characteristics obtained for the PLEDs with ZnO nanoparticles of diameter  $\leq 50$  nm incorporated in 150 nm MEH-PPV matrix. Addition of ZnO particles results into a significant linear decrease of opening bias while increases the electroluminescence intensity of the device operated at 10 V.

### 5.3.2 Nanocomposite diodes with undoped ZnO particles $\leq 15$ nm

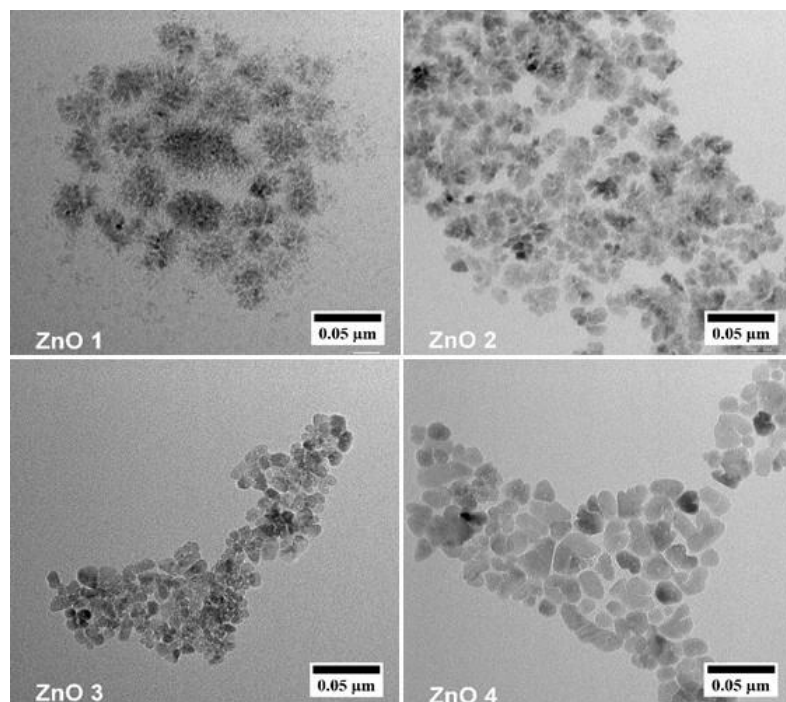


Figure 7 TEM micrographs of ZnO nanoparticles prepared from solutions with various precursor concentration. The average size of particles is 4, 8, 11, and 14 nm for samples ZnO 1, 2, 3 and 4, respectively.

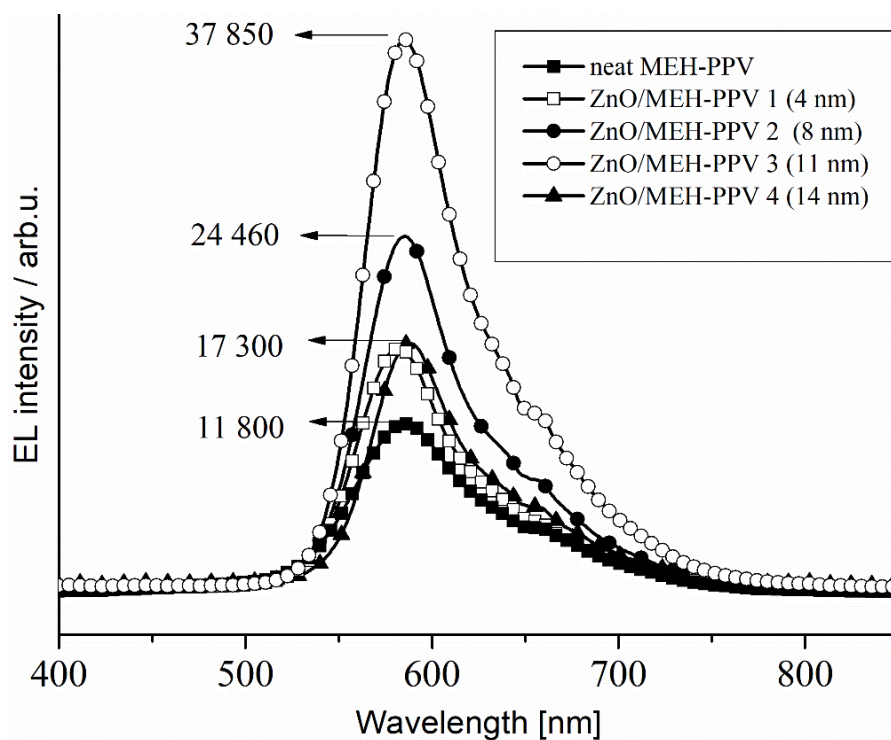


Figure 8 Intensity of electroluminescence of PLED devices with different size of nano ZnO in the active layer, input voltage 10 V and 1s integration time

Table 4 summarises the main characteristics of prepared PLEDs with ca 35 nm thick active nanocomposite layer prepared with ZnO nanoparticles of varying diameter. The decrease in opening bias in comparison with the neat polymer-based device was confirmed for nanoparticle addition; however, a clear trend with decreasing particle size was not observed. On the other hand, electroluminescence intensity has its maximum for nanoparticles with the diameter ca 11 nm. It can be hypothesized, that the effects of smaller particles are limited due to strong quantum confinement, which imposes large strain on the eventual occurrence of excitons in the particle. Moreover, the lifetime of excitons is known to be reasonably shortened due to strong quantum confinement which is another limiting factor of the ability of the nanoparticle to be involved in charge transfer processes in the polymer matrix. According to the emission spectra, the electroluminescence is a result of radiative recombination between electrons and holes in MEH-PPV polymer matrix, and the 0–0 relaxation path is preferred [11, 13].

*Table 4 Highlighted parameters of PLEDs with ZnO nanoparticles incorporated in 35 nm thick nanocomposite layer with MEH-PPV matrix.*

<b>The diameter of ZnO NPs in MEH-PPV [nm]</b>	<b>opening bias [V]</b>	<b>EL intensity maximum powered by 10 V [arb.u.]</b>
4 ± 1	4.9	17 300
8 ± 1	4.2	24 500
11 ± 2	5.0	37 900
14 ± 3	5.1	17 300
neat MEH-PPV	5.5	11 800

### **5.3.3 Nanocomposite diodes with Fe doped ZnO nanoparticles**

Doping of ZnO by Fe typically leads to the decrease of the bandgap and enhances separation of the exciton into free charge carriers. On the other hand, the newly created states in the bandgap may act as traps for electrons as well as for holes.

In our case, a series of Fe doped nanoparticles dispersed in toluene was prepared for incorporation into the nanocomposite active layer. The Fe dopant concentration varied from 2 up to 10 at% (expressed as a ratio of Fe concentration to the total concentration of Fe and Zn in the Fe:ZnO material, in other words, it is the coefficient x in the formula  $Fe_xZn_{(1-x)}O$ ) as analysed by EDS and in good agreement with the initial composition of the reaction mixture. Incorporation of the Fe dopant was homogenous and mainly  $Fe^{2+}$  states were formed in spite of the use of ferric source compound. It is expected that the Fe(+III) was reduced to Fe(+II) by the diethylene glycol used in the microwave-assisted solvothermal

synthesis. The prevalence of  $\text{Fe}^{2+}$  was revealed by XPS. The size of particles varied insignificantly from 11 to 14 nm as confirmed by XRD and TEM. The microscopic images captured by TEM are presented in Figure 9. The undoped ZnO particles of 11 nm in diameter were used as the reference [13].

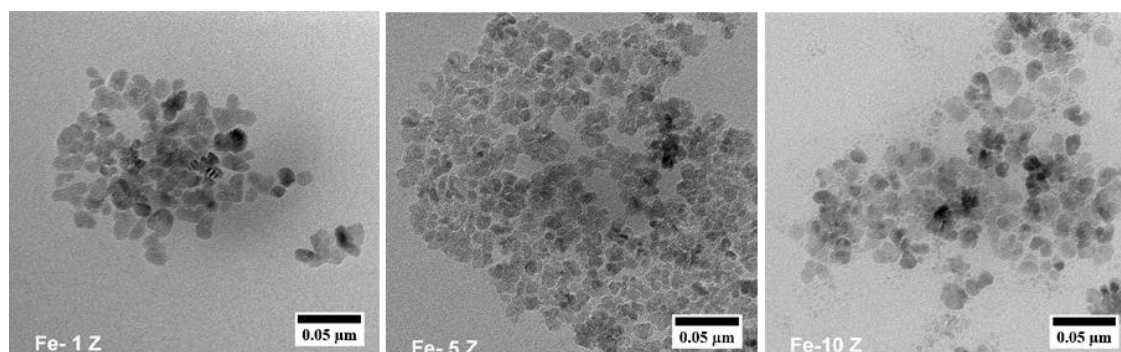


Figure 9 TEM images of  $\text{Fe}_x\text{Zn}_{(1-x)}\text{O}$  nanoparticles

The size and bandgap of the nanoparticles are summarised in Table 5. A significant decrease in the bandgap was caused by the Fe doping. All prepared particle samples showed UV photoluminescence only testifying for the presence of Zn interstitials while no significant manifestation of states related to the oxygen vacancies either in volume or on the surface was observed in visible emission range. Thus, surface defects were most likely passivated by the capping agent. No luminescence in the visible range was observed for doped samples although pronounced tailing up to 500 nm was observed by UV–Vis and DRUV–Vis [13].

Table 5 Basic properties of Fe doped nanoparticles.

Nanoparticle sample type; code	Band gap [eV]	TEM size [nm]
Fe:ZnO (2% of Fe in ZnO); Fe-1 Z	3.0	$14 \pm 3$
Fe:ZnO (5% of Fe in ZnO); Fe-5 Z	2.7	$11 \pm 2$
Fe:ZnO (10% of Fe in ZnO); Fe-10 Z	2.6	$13 \pm 3$
ZnO	3.2	$11 \pm 2$

The effect of Fe doping level in ZnO nanoparticles incorporated into the nanocomposite active layers in tested devices can be the characteristics of the devices with neat MEH-PPV and undoped ZnO/MEH-PPV active layers. All prepared devices with  $\text{Fe}_x\text{Zn}_{(1-x)}\text{O}$ /MEH-PPV have similar I–V characteristics in terms of shape and values. The opening bias of neat MEH-PPV device is around 5.5 V, and that of ZnO/MEH-PPV is approximately 5.0 V. The PLED devices with Fe-1 Z, Fe-5 Z and Fe-10 Z nanocomposite active layers exhibited opening bias about 3.5 V, 3.0 V and 2.8 V, respectively.

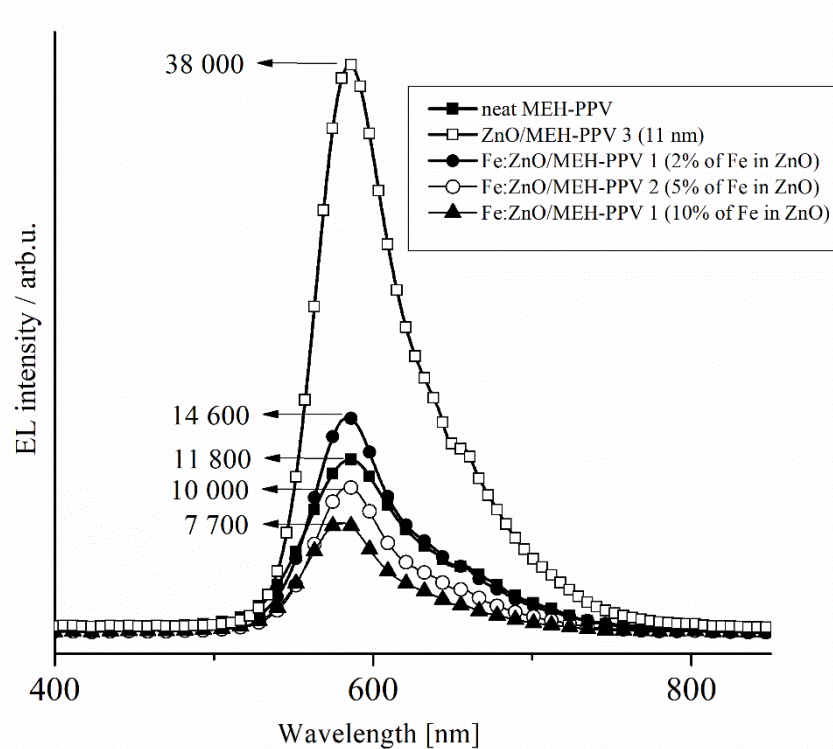


Figure 10 EL intensity of devices with Fe:ZnO at 10 V and 1s integration time

The electroluminescence spectra of prepared devices are in Figure 10. A decrease in EL emission peak maxima intensity with increasing Fe dopant concentration was observed. According to the typical shape of the emission spectra, the electroluminescence is a result of radiative recombination between electrons and holes in MEH-PPV polymer matrix and the 0–0 relaxation path is preferred.

Table 6 Highlighted parameters of PLEDs with Fe: ZnO nanoparticles incorporated in 35 nm thick nanocomposite layer with MEH-PPV matrix.

Nanocomposite sample type	opening bias [V]	EL intensity maximum [arb.u.]
Fe:ZnO/MEH-PPV 1 (2% of Fe in ZnO)	3.5	14 600
Fe:ZnO/MEH-PPV 2 (5% of Fe in ZnO)	3.0	10 000
Fe:ZnO/MEH-PPV 3 (10% of Fe in ZnO)	2.8	7 700
ZnO/MEH-PPV 3 (11 nm)	5.0	38 000
neat MEH-PPV	5.5	11 800

The EL intensity maximum values are summarised in Table 6, together with the values of the opening bias. It can be clearly seen, that the EL intensity decreases significantly with the increase of the doping level. Actually, it is the sample containing undoped ZnO which has the highest luminescence efficiency

when forwarded by 10 V. Samples prepared from nanoparticles with higher doping concentrations have EL intensity maximum even lower than that of the reference neat MEH-PPV polymer sample. On the other hand, Fe doping decreases the opening bias significantly; thus, it opens a way to a compromise between these two effects and finding of an optimum power efficiency even in this case.

### 5.3.4 Nanocomposite diodes with Al-doped ZnO nanoparticles

Doping of ZnO by Al which is an element belonging to the leading group of elements (a post-transition metal) results typically to the increase of the bandgap width up to 4.1 eV and incorporation of the trivalent aluminium results in n-doping of the ZnO semiconductor. Conductivity, mobility of carriers and their concentration are typically increased with increasing Al dopant concentration. The contradiction between the bandgap widening and the increase in the n-type conductivity at the same time might be attributed to the fact that no local energy level is produced due to Al incorporation connected with immediate transferring of the extra electron into the conductive band. On the other hand, the success of doping is tightly connected with the used method of the material preparation and hydrothermal processes employing co-precipitation result usually into phase separation of aluminate production. Therefore, high-temperature physical doping methods or organic precursor based solvothermal methods are used for the synthesis of Al-doped ZnO materials. A bandgap shrinkage can also be observed due to the increased material disorder and increased oxygen vacancy concentration caused by the method of material preparation. The microscopic images captured by TEM are presented in Figure 11.

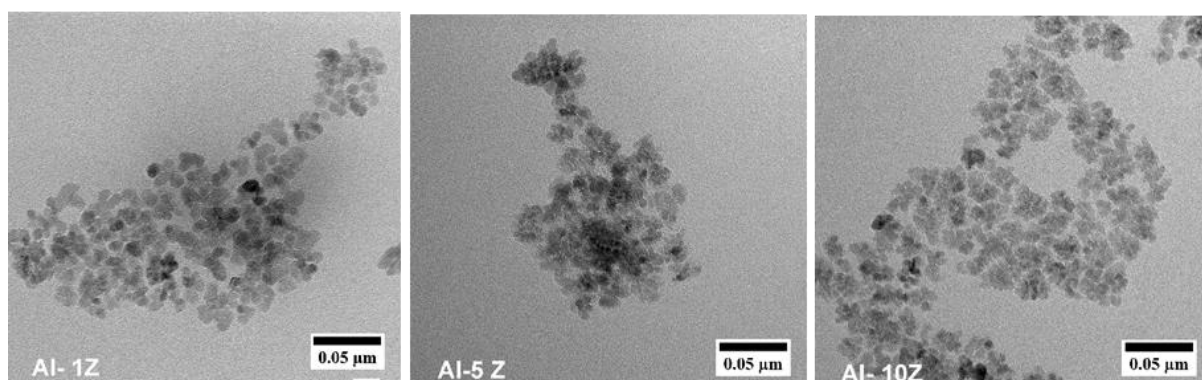


Figure 11 TEM images of  $Al_xZn_{(1-x)}O$  nanoparticles

In our case, a series of Al-doped nanoparticles dispersed in toluene was prepared for incorporation into the nanocomposite active layer. The Al dopant concentration varied from 1 up to 10 at% (expressed as a ratio of Al concentration to the total concentration of Al and Zn in the Al:ZnO material, in other words, it is the coefficient  $x$  in the formula  $Al_xZn_{(1-x)}O$  as analysed by EDS and in relatively good agreement with the initial composition of the reaction mixture. Incorporation of the Al dopant was homogenous, and no other phases were

formed. The size of particles varied insignificantly from 9 to 8 nm as confirmed by XRD and TEM. The microscopic images captured by TEM are presented in Figure 18. The undoped ZnO particles of 11 nm in diameter were used as the reference.

*Table 7 Basic properties of Al doped nanoparticles.*

<b>Nanoparticle sample type; code</b>	<b>Band gap [eV]</b>	<b>TEM size [nm]</b>
Al:ZnO (1% of Al in ZnO); Al -1 Z	3.1	9 ± 2
Al:ZnO (5% of Al in ZnO); Al -5 Z	3.1	9 ± 2
Al:ZnO (10% of Al in ZnO); Al -10 Z	3.2	8 ± 2
ZnO	3.2	11 ± 2

The size and bandgap of the Al-doped ZnO nanoparticles are summarised in Table 7. No significant variation of the bandgap or particle size was caused by the Al doping. As in the case of Fe doping, all prepared particle samples showed UV photoluminescence only while no significant manifestation of states related to the oxygen vacancies either in volume or on the surface were observed in visible emission range. Thus, surface defects were most likely passivated by the capping agent if they were present at all. The PL emission maximum showed remarkable blue shift with doping, unlike the bandgap width, which might be related to the change of the absorbance maximum blue shift observed with increasing concentration of Al in prepared nanoparticles. No tailing into visible range was observed; thus, no significant influence of traps is expected to have a direct impact on eventual electroluminescence of nanocomposites containing these particles. The effect of Al doping level in ZnO nanoparticles incorporated into the nanocomposite active layers in tested devices can be followed from the same set of experimental investigations as in previous cases. (To note 50 wt%, i.e. 15 vol% of particles in prepared nanocomposites.) The Current-voltage (I–V) characteristics of the PLED under the forward bias varied from 0 V up to 10 V are depicted in Figure 12. The characteristics of the device with neat MEH-PPV and undoped ZnO/MEH-PPV active layers differ significantly from the characteristics of all prepared devices with  $\text{Al}_x\text{Zn}_{(1-x)}\text{O}$ /MEH-PPV as active layers. These three devices have similar I–V characteristics in terms of shape and values. The opening bias of neat MEH-PPV device is around 5.5 V, and that of ZnO/MEH-PPV is approximately 5.0 V. All PLED devices with aluminium doped ZnO nanoparticles exhibited ca the same opening bias about 2.8 V.

The electroluminescence spectra of prepared devices are in Figure 13. A significant increase in EL emission peak maxima intensity with increasing Al dopant concentration was observed. According to the typical shape of the emission spectra, the electroluminescence is a result of radiative recombination between electrons and holes in MEH-PPV polymer matrix and the 0–0 relaxation path is mainly preferred while 0-1 relaxation path is mostly suppressed.

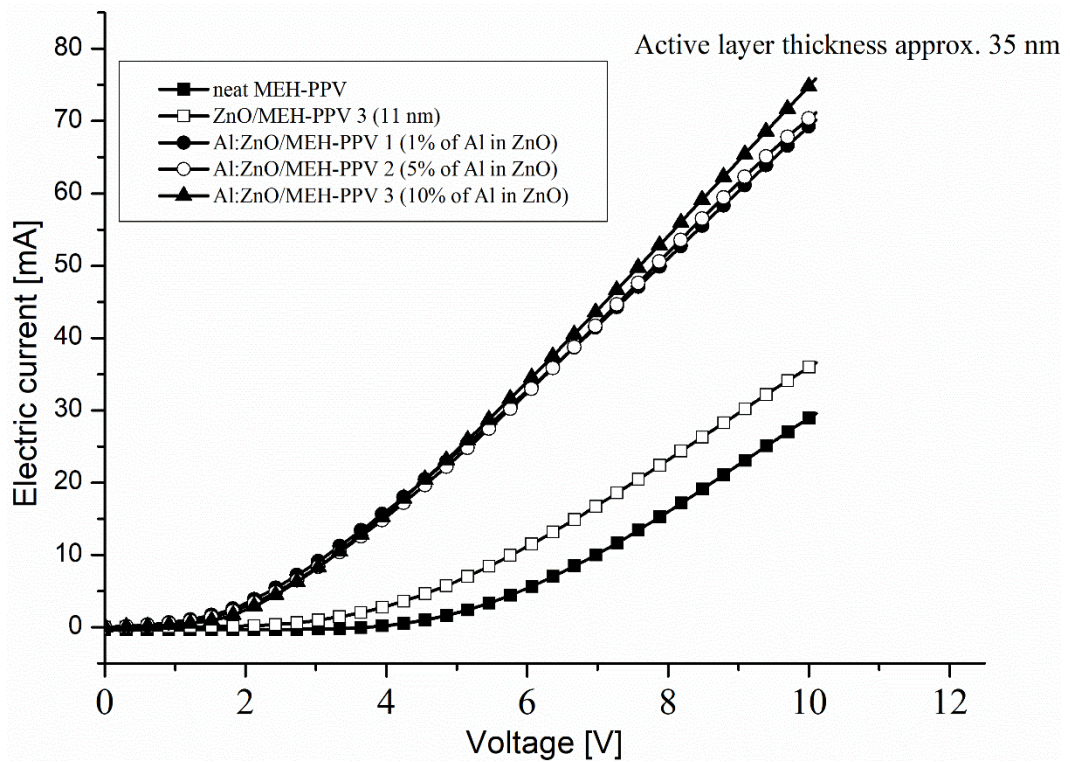


Figure 12 I-V characteristic of PLEDs with  $Al_xZn_{(1-x)}O/MEH-PPV$

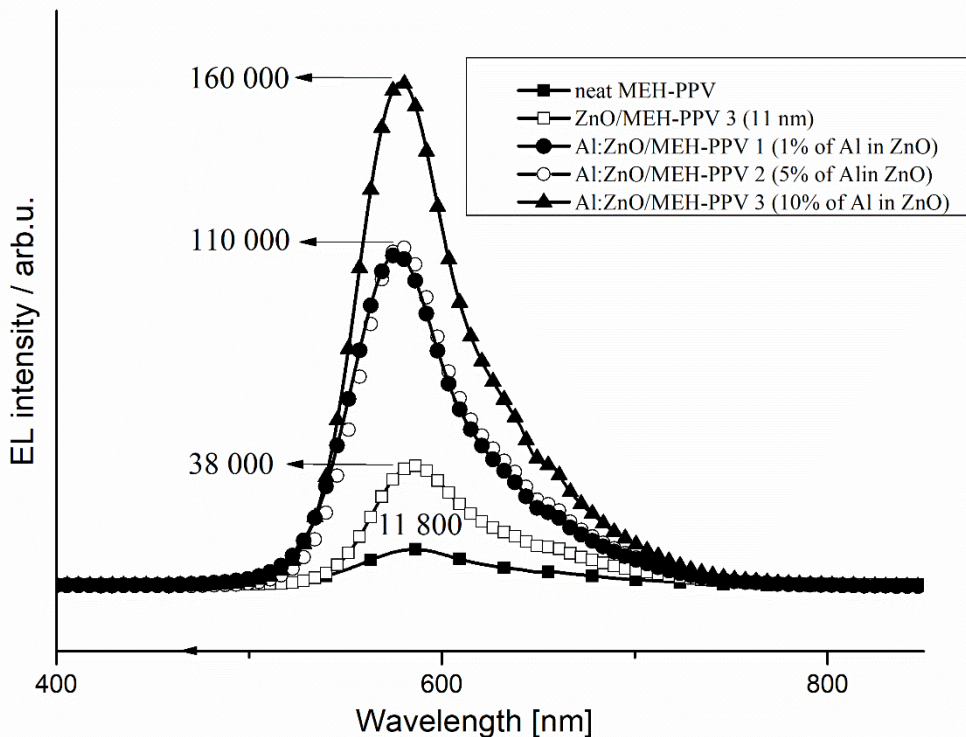


Figure 13 EL intensity of devices with Al:ZnO at 10 V and 1s integration time

The EL intensity maximum values are summarised in Table 8, together with the values of the opening bias. It can be clearly seen, that the EL intensity

increases significantly with the increase of the doping level. Actually, the sample Al – 10 Z has 4 times higher EL intensity than the sample containing undoped ZnO and 15 times higher than the neat MEH-PPV reference when forwarded by 10 V. On the other hand, Al doping decreases the opening bias significantly but independently on the doping level, thus it opens a way to a very reliable enhancement of PLEDs performance using studied type of particles.

*Table 8 Highlighted parameters of PLEDs with Al: ZnO nanoparticles incorporated in 35 nm thick nanocomposite layer with MEH-PPV matrix.*

<b>Nanocomposite sample type; code</b>	<b>Opening bias [V]</b>	<b>EL intensity maximum [arb.u.]</b>
Al:ZnO (1% of Al in ZnO); Al -1 Z	2.8	110 000
Al:ZnO (5% of Al in ZnO); Al -5 Z	2.8	110 000
Al:ZnO (10% of Al in ZnO); Al -10 Z	2.8	160 000
ZnO/MEH-PPV 3 (11 nm)	5.0	38 000
neat MEH-PPV	5.5	11 800

## 5.4 Performance of prepared devices

To analyse and discuss the performance of prepared devices, their performance should be expressed in terms of luminance and current efficiency. Such an approach enables comparing the performance of prepared PLEDs not only within the series of experiments in this dissertation but also with the data reported throughout the scientific literature published on similar issues. Nevertheless, it is somewhat problematic to compare diodes with different opening voltages and operated at various conditions.

Table 9 summarised recalculated performance indicators for all prepared and tested samples. The current density  $J$  is obtained as current per area, which is read from I-V characteristics of the devices at the forward bias 10 V. Current efficiency,  $CE$ , is the ratio of the luminance  $L_{vPLED}$  and the current density.

It should be reminded, that the values in Table 9 represent the lowest reasonable estimation of the luminance and current efficiency of prepared devices, which was possible to obtain under given conditions. Nevertheless, the comparison with literature is of particular value. Among many reports, the work of Alam M. M. et al. [14] from the beginning of the millennium can be cited as a perfect example. The authors used a single-layer ITO/MEH-PPV- (45 nm)/Al diode as a primary reference device in their research. This diode had a turn-on voltage (opening bias) of 12 V and a luminance of 163 cd/m<sup>2</sup> at 15.5 V and a current density of 5000 A/m<sup>2</sup>. The standard diodes prepared within the research work presented in this dissertation can be classified as of superior quality in comparison with the cited results. The performance of our prepared diodes is at

least one by one order of magnitude higher, while the current density is almost the same, but a lower forward bias was used. Alam and his co-authors reported the preparation of many other multi-layered devices with supporting layers imparting enhanced luminance to these devices. They achieved luminances several times higher than that of their single MEH-PPV layer-based device. The introduction of a poly-(ethylenedioxythiophene)/poly(styrenesulfonic acid) hole injection layer (PEDOT:PSS) onto the anode resulted in an increase of the luminance to 220 cd/m<sup>2</sup>. The subsequent application of a poly(p-phenylenebenzobisthiazole) electron injection layer (PBZT) under the aluminium cathode resulted in a reasonable increase of the luminance up to 1200 cd/m<sup>2</sup> and large enhancement of the efficiency of the diode. In general, they reported the importance of supporting layers on the external quantum efficiency and optimised the devices from this point of view. Unlike this approach, this work entirely focuses on the study and development of the active layer itself, keeping the structure of the diode as simple as possible, yet with the hole blocking layer. The casting procedure of the MEH-PPV was optimised, and magnesium was used as a cathode instead of aluminium [15], because magnesium is the best choice among non-oxidizing metals due to its lowest work function.

*Table 9 Summary of performance of prepared PLEDs measured @ 10V.*

<b>Sample type</b>	<b>Luminance, <math>L_{vPLED}</math>, [cd/m<sup>2</sup>]</b>	<b>Current efficiency, <math>CE</math>, [cd/A]</b>	<b>Current density, <math>J</math>, [A/m<sup>2</sup>]</b>
neat MEH-PPV (30 nm)	1 900.00	0.37	5 200.00
neat MEH-PPV (45 nm)	2 000.00	0.30	6 600.00
neat MEH-PPV (80)	640.00	0.96	670.00
neat MEH-PPV (100)	280.00	0.50	560.00
neat MEH-PPV (150) under 15V	70.00	0.08	890.00
comerc.ZnO (50 nm)/MEH-PPV 1:1	1 600.00	2.06	780.00
ZnO (4 nm)/MEH-PPV (35 nm) 1:1	2 200.00	0.35	6 200.00
ZnO (8 nm)/MEH-PPV (35 nm) 1:1	3 300.00	0.41	8 100.00
ZnO (11 nm)/MEH-PPV (35 nm) 1:1	5 100.00	0.63	8 100.00
ZnO (14 nm)/MEH-PPV (35 nm) 1:1	2 200.00	0.25	8 700.00
FeZnO/MEH-PPV (2% of Fe in ZnO)	1 900.00	0.17	11 200.00
FeZnO/MEH-PPV (5% of Fe in ZnO)	1 300.00	0.15	8 700.00
FeZnO/MEH-PPV (10% of Fe in ZnO)	1 000.00	0.12	8 100.00
AlZnO/MEH-PPV (1% of Al in ZnO)	13 900.00	0.81	17 100.00
AlZnO/MEH-PPV (5% of Al in ZnO)	14 000.00	0.86	16 200.00
AlZnO/MEH-PPV (10% of Al in ZnO)	20 700.00	1.31	15 800.00

During the last two decades, the field has grown amazingly, and the attention was paid mainly to the studies, development, and optimisation of the supporting layers on both poles of the device. The number of layers and sophistication of the multi-layered structure of a typically reported device significantly increased. Efficient hole blocking and electron injection buffer layers on the side of the cathode [16] and hole injection and electron blocking layers as well as surface modifications on the side of the ITO anode [17, 18] allowed achievements of luminances of MEH-PPV and other polymer-based devices about 20 000 cd/m<sup>2</sup> with current efficiencies from tenths to a few units cd/A. According to the recent literature, it seems that the brightness (luminance) of PLEDs does not increase much progressively, and the attention is focused on the research of strategies on how to tune hole and electron currents and achieve balanced electron and hole injection to the emissive layer. While the maximum luminance of reported diodes is about a few tens of thousands of cd/m<sup>2</sup>, the current efficiency grows up to tens cd/A. Indeed, the luminance of standard LED displays, which is typically in the order of several hundreds of cd/m<sup>2</sup> has been already achieved and seems to be sufficient for most of the applications, while the challenge is the increase of the external efficiency of the PLEDs. The trend towards studies and development of all-solution-processed PLEDs is also notable. [19-21]

Very recently, the attention turned out to the large area lighting panels and general lighting, which invokes a need for technologies for the fabrication of low-cost and large-area flexible devices with extremely high brightness. Luminances about 100 thousands of cd/m<sup>2</sup> are reported [22, 23]. The research strategy follows the general direction of building-up multi-layered supporting thin films, including zinc oxide nanoparticles and quantum dots incorporation into the device structure [24-27].

Direct incorporation of nano ZnO particles into a nanocomposite active layer with MEH-PPV matrix is used to improve the luminance of prepared devices in this work. The electroluminescent spectra recorded for all samples of prepared diodes confirmed that the radiative recombination proceeds only on the MEH-PPV polymer chains. No emission associated directly with transitions in ZnO was observed. The electroluminescence spectra of neat MEH-PPV show the thinner the active layer is, the more is the 0-0 radiation channel preferred for emission. The addition of large nanoparticles ( $\leq 50$  nm) to the thickest layer did not cause a change of the ratio between the main emission peak and the long-wavelength shoulder as documented in Figure 6.

Figure 14 illustrates the band structure and working principle of the prepared diodes based on neat MEH-PPV (left side) as well as nano ZnO/MEH-PPV nanocomposite (right side). In both cases, the electrons injected directly from the Mg cathode into the emission layer must overcome a potential barrier, as illustrated by the path e1 in the Figure. Due to the simple design of the device, there is no other supporting layer which could facilitate the transport of the electron on the polymer chain. Due to the presence of the nano ZnO particles,

the electron injection could follow the path **e2** which should be energetically favoured, but is not barrier-less, since there is no direct contact between the particle and the Mg cathode. The conduction band of ZnO lies only 0.5 eV below the Fermi level of the cathode.

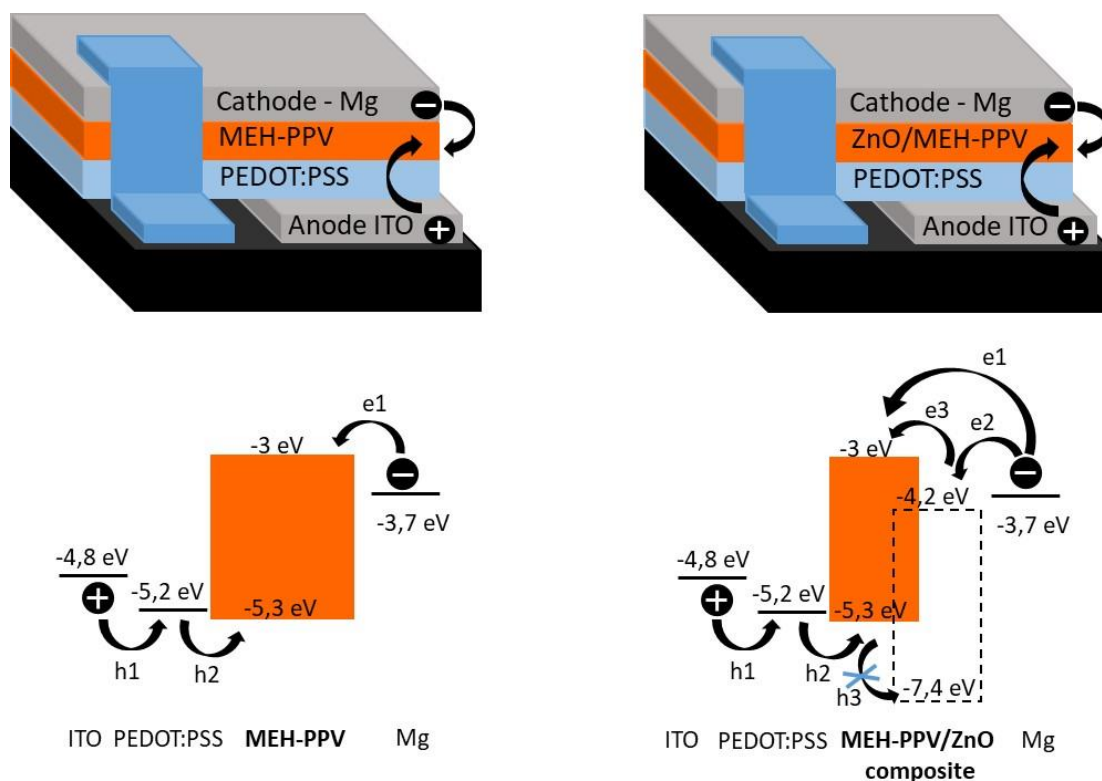


Figure 14 Comparison of band structure of prepared polymer and nanocomposite light-emitting devices.

On the other hand, the filling by 15 vol% of nanoparticles in size about 10 nm approaches the total percolation of the total matrix volume for hopping and tunnelling transport (judged on the simple geometry considerations only). Enhancement of transport mechanisms through conductive bands of nano ZnO is possible through the path **e3**, which has a slightly higher barrier than **e1**, but it may occur on much larger surface of the nanoparticle polymer interface. Moreover, electrons transferred through the path **e3** can be easily replenished via the path **e2**.

The design of the pathway for holes is a standard of its kind. The ITO anode is covered by a hole injection PEDOT:PSS layer, which is applied in a thickness of 30-40 nm to all prepared devices. The hole injection is facilitated through a cascade of **h1** and **h2** pathways ending-up in the HOMO of MEH-PPV (valence band) which is a typical p-conductive material. Presence of ZnO creates an additional barrier to the transport of holes due to the large difference between the ZnO valence band energy and the HOMO energy of MEH-PPV excluding thus **h3** from eventual action.

The effect of doping of the nanoparticles on the properties can be explained within the standard interpretational framework for the doping of semiconductors, yet in the nanoparticle form [13, 28-30].

Doping of ZnO by Fe causes the population of fixed acceptor states above the valence band of the ZnO, leaving free holes in the valence band. As a result, the optical bandgap is narrowed significantly, while the valence band can be shifted upward on the energy scale to be closer to the HOMO level of the MEH-PPV. Thus, the barrier for **h3** pathway is reduced. On the other hand, the addition of Fe-doped particles to the emissive layer resulted in a significant decrease of the opening voltage.

The negative doping of ZnO nanoparticles by Al populates shallow fixed states nearby the conduction band and free electrons in the conduction band. However, the optical bandgap did not change, and no tailing was observed. Instead, a blue shift was observed for the photoluminescence of the doped nanoparticles. It means, that although some states in the conduction band are filled, this blocking might be compensated by the perturbation of the bandgap and the level of the conduction band available to the free conductive electrons is lifted upwards on the energy scale, which is somewhat closer to the LUMO of MEH-PPV promoting thus the **e3** pathway. Unlike electron pathways, the barrier for **h3** remains unchanged by the n-doping and contributes positively to the charge carrier transfer balance and overall performance of the devices. As a result, a significant enhancement of the electroluminescence is observed as well as improved current efficiency.

## 6. CONCLUSIONS

The research presented in this doctoral thesis aimed at preparation of nanocomposite thin films based on bandgap engineered ZnO nanoparticles as a filler and standard conductive polymer poly[2-methoxy-5-(2-ethylhexyloxy)-1,4-phenylenevinylene] (MEH-PPV) as a matrix. Thence such films were used and studied as the active layer in polymer light-emitting diodes (PLEDs). The intention of the embodiment of prepared nanocomposite material into the functional PLED was to improve its performance in terms of luminance intensity, lowering of bias voltage (turn-on voltage), and luminance efficiency.

-----

According to this concept, appropriate steps have been taken to reveal the full potential of studied polymer/inorganic nanocomposites. Firstly, it was necessary to understand and master the behaviour of used native conjugated materials MEH-PPV in terms of processing properties such as solubility and ability to form thin films. Although it is a very well known and most frequently studied model polymer material, besides mastering its use, new knowledge was also gathered. Series of thin films with varying thickness of the conjugated polymer was prepared on selected substrates and examined by complementary methods (PL, profilometry, UV-VIS, Surface photovoltaic effect etc.) in order to complete and confirm previous results.

As the next step, the primary effects of nanoparticle addition on the band structure of prepared nanocomposite thin films were studied with the aid of energy-resolved electrochemical impedance spectrometry. The obtained density of states (DOS) data confirmed the success of the intention of bandgap tailoring. Photoluminescence measurements allowed for completing the analysis of the prepared nanocomposite thin film structure by comparison of their photoluminescence spectra with the photoluminescence spectra of the thin films made from the neat MEH-PPV films. Addition of undoped ZnO to the MEH-PPV matrix slightly increases the structural disorder of the polymer (increases deep defect concentration in the bandgap by one order of magnitude) in the prepared thin films as well as (hypothetically) contributes to a decrease of photoluminescence due to the photoinduced electron transfer from the LUMO of MEH-PPV to the conduction band of the ZnO semiconductor. The latter effect may be reversible in the case of an electroluminescent device and can contribute to the increase of luminance of such an LED. The addition of the Fe-doped ZnO to the MEH-PPV matrix results in a decrease in the overall intensity of the photoluminescence of prepared thin films. Positively doped particles provide an alternative pathway for the relaxation of excited electrons due to recombination of interfacial charge transfer exciton. In the case of the most heavily Fe-doped ZnO, there is observable a strong quenching in the whole range of emission. So, the incorporation of this system (denoted 15 % atomic, or  $\text{Fe}_{0.15}\text{Zn}_{0.85}\text{O}$ ) to the light-emitting diodes was not considered. The Al-doped ZnO incorporated into

MEH-PPV polymer matrix shows an increase in photoluminescence intensities in the whole emission interval compared to other thin-film layers. Aluminium is a negative dopant for ZnO and changes the conductivity band structure of the nano ZnO in such a way that it is more aligned to the LUMO of the polymer. Indeed, more pronounced increase of density of states nearby LUMO of the polymer was observed for Al-doped ZnO nanoparticles than for neat ZnO nanoparticles due to the increase of the n-doping ability of the doped nanoparticles with respect to the MEH-PPV polymer. Moreover, the density of deep states near HOMO of the polymer is decreased even in comparison with the neat MEH-PPV film most likely due to the filling of the traps usually present in the bandgap of the cast polymer of such thickness.

-----

Achieved experience and knowledge from the studies on neat polymer thin films, was then used for fabrication of standard PLEDs with the emphasis on the MEH-PPV active layer thickness, other parameters such as the material of electrodes and supporting layers, their thickness, and order in the device were kept as constant. The I-V characteristics and intensity of electroluminescence of prepared devices were recorded and analysed to demonstrate the behaviour of devices with active layer thickness below 150 nm, which is a critical threshold value for structural ordering development. The standard neat MEH-PPV diode with the thickness of the active layer about 30 nm was chosen for use as the reference.

-----

Based on inspirations taken from the literature and on the new knowledge gathered from original experiments with the nanocomposite thin films, the focus in preparation of PLEDs was then turned to the implementation of inorganic nanoparticles into the PLEDs structure. The majority of reports in available scientific papers dealt with the deposition of inorganic nanoparticles in the form of a separate layer before casting the active polymer solution [31, 32]. Such an approach leads to the achievement of better device performance; the thin layer from ZnO nanoparticles has a positive effect on the electron injection into the active layer from the cathode. Simultaneously, due to wide band-gap, the ZnO layer blocks the positive charge carriers and increases the probability of recombination of electrons and holes on the active layer. Nevertheless, the procedure of making such a device is quite complicated and demanding on used experimental equipment. Thus, the idea of simple incorporation of the nanoparticle filler directly into the active layer has arisen. A series of nanocomposite thin films were prepared using commercially available ZnO nanoparticles. These layers were characterised using available methods and included in the PLEDs system with the emphasis of concentration of ZnO nanoparticles in MEH-PPV matrix. Commercially available particles were chosen for the first experiments. Because of the big particle size ( $\leq 50$  nm), the active layer of 150 nm thickness was prepared. The I-V characteristics and

intensity of electroluminescence of prepared devices were analysed. It was confirmed, that the addition of ZnO nanoparticles improves the characteristics of prepared diodes significantly. However, the size of the particles was too big and requested the application of the thickest polymer layer, which has the worst performance among tested thin films. Moreover, the diameter of the nanoparticles is such, that only weak quantum confinement effects can be manifested (if any at all) and much more pronounced effects should be observed if smaller particles are used. Nevertheless, viability of 50 wt% (15 vol%) filling of the nanocomposite thin layer was proven, and the 1:1 weight ratio between the nanoparticulate filler and polymer matrix was used throughout all next series of experiments.

-----

At about the same time, my colleagues from our research group were able to synthesise zinc oxide nanoparticles of controllable size at a suitable nano-dimension scale. The availability of such particles allowed the application of 4, 8, 11 and 14 nm ZnO nanoparticles into the MEH-PPV matrix. Therefore, it was also possible to reduce the thickness of the prepared nanocomposite active layer to approx. 35 nm. The same approaches for preparation and set of characterisations were applied as in the previously mentioned case, and a series of PLEDs with a constant concentration of synthesised nanoparticles, but with different diameter was then prepared and studied. As the main result, an optimum size of ZnO nanoparticle at about 11 nm was found to be most effective for application in prepared PLEDs both in terms of luminance intensity and opening bias lowering. The results of this study were already partially published [33].

-----

The next challenge was to attempt the synthesis and application of nanoparticles that could compete with or overcome the existing PLEDs performance. The initial idea of utilisation of ZnO nanoparticles incorporated in the conjugated polymer matrix has been successfully tested, as described above. An approach involving doping of zinc oxide with positive and negative dopants was conceived to make the step beyond the common ambits. Control over the doping process of ZnO nanoparticles allowed engineering of the bandgap of doped material and opened up a new option for synthesising of inorganic nanomaterials in our laboratory with properties tailored as needed on demand. In this regard, the whole series of nanoparticle syntheses have been performed with respect to the type and concentration of dopant in the zinc oxide. Besides the neat ZnO nanoparticles, the Fe- and Al-doped ZnO nanoparticles were prepared and implemented in PLEDs from which results obtained on Fe-doped ZnO/MEH-PPV nanocomposites are already published [13]. A new manuscript on Al-doped ZnO nanoparticle incorporation to MEH-PPV based PLEDs is in the stage of first draft preparation. It can be generalised, that the positive Fe-doping decreases the maximum luminance of the diode at the given operating voltage in comparison with the reference undoped ZnO nanocomposite; however, it also reduces the

opening bias significantly. Thus, Fe-doping opens a way how to optimise the power efficiency of prepared devices by balancing these two effects. On the contrary, the use of negative Al-doping of ZnO nanoparticles resulted in a much more valuable success. All Al-doped nano ZnO containing samples largely surpassed the reference undoped ZnO system. Thus, significant enhancement of the opening bias and luminance of the prepared PLEDs was achieved.

## **7. CLOSING REMARK**

### **7.1 Contribution to science and practice**

Nowadays, the area of polymer electronics is one of the speedy growing industry fields. Polymer conductive thin films can be used in applications such as flexible imaging devices, displays, and light-emitting devices or there, where the handling of conventional materials was impossible. Polymer conductive thin films can be applied in photovoltaics as well. However, the properties and durability of conjugated conductive polymers are often limited; hence, it is favourable to dope them by additives or fillers and thus to prepare composite materials which have improved optoelectrical properties, stability, and efficiency. Among these paramount of organic electronics, it was the search for long-lasting highly intensive light sources, which motivated the presented study of ZnO/MEH-PPV nanocomposite thin films applied as active layers in PLEDs.

It is hard, to fulfil all the often contradictory requirements laid on the material for application as an active layer in high-performance LEDs. Therefore, the obtained experimental results of the use of bandgap engineered doped nano ZnO/MEH-PPV (poly[2-methoxy-5-(2-ethylhexyloxy)-1,4-phenylenevinylene]) are of general importance. A new simple and viable preparation strategy of thin nanocomposite films was exemplified by the application of these films as active layers into the PLEDs. Although a model polymer MEH-PPV was used as a matrix, the findings embodied in this dissertation have straightforward implications for the construction of real devices with industrial-scale application potential. The influence of the nanoparticle size and composition, the thickness of thin films and parameters during their preparation on the optoelectronic properties and PLEDs performance were described. Electronic structure of such nanocomposite films was studied with energy-resolved electrochemical impedance spectroscopy for the first time in the world. Addition of any of the studied nanoparticles enhanced the luminance of prepared devices in comparison with reference samples made from neat MEH-PPV polymers. Nanoparticle concentration, size and thin film thickness optimum was found for pure ZnO system within the range of tested parameters. As the main achievement, two principally different dopants – iron and aluminium – were used to modify the bandgap of the material and effects of concentration of the dopants in nanoparticles was investigated. The Fe-doping decreases the maximum luminance of the diode at the given operating voltage in comparison with the

reference undoped ZnO nanocomposite; however, it also decreases the opening bias significantly. Thus, Fe-doping opens a way to a search for the best balance between these two effects to optimize the power efficiency of prepared devices. Significant enhancement of all examined performance parameters in comparison with the reference undoped ZnO system was achieved for Al-doped nano ZnO containing samples. Both the opening bias and luminance of the diode were significantly enhanced by using this material tailored in our laboratory.

## 7.2 Ongoing research and future prospective

Based on the achieved results, the current research is focused on the incorporation of prepared nanoparticles to the different conjugated polymer, namely F8BT, which is a representative of a p-conductive polymer with real application records from the electronics industry.

For completeness and confirmation of the positive effect of doping and thus the use of nanocomposite layers in PLEDs, the stability and life-time measurement must be additionally performed. Simultaneously, the electroluminescence intensity measurement should be better carried out under the constant electric current flows through the device.

From a practical point of view, the improvement of luminance, stability and external quantum efficiency of devices prepared in our laboratories can play a significant role in the technology transfer from laboratory to real applications. On the lightning market, demand for lightweight, well designed and personalised product exists. Polymer light-emitting devices with high efficiency could satisfy such a requirement.

## REFERENCES

- [1] HAN, J. W., JOO, C. W., LEE, J., LE, D. J., KANG, J., YU, S., SUNG, W. J., CHO, N. S. and KIM, Y. H. Enhanced outcoupling in down-conversion white organic light-emitting diodes using imprinted microlens array films with breath figure patterns. *Science and Technology of Advanced Materials* [online]. 2019, vol. 20, no. 1, p. 35-41. ISSN 1468-6996.
- [2] BRÜTTING, Wolfgang. *Physics of organic semiconductors*. 2., compl. new rev. ed. Weinheim: Wiley-VCH, 2012. ISBN 9783527410538.
- [3] SUN, Y., WANG, W., ZHANG, H., SU, Q., WEI, J., LIU, P., CHEN, S. and ZHANG, S. High-Performance Quantum Dot Light-Emitting Diodes Based on Al-Doped ZnO Nanoparticles Electron Transport Layer. *Acs Applied Materials & Interfaces* [online]. 2018, vol. 10, no. 22, p. 18902-18909. ISSN 1944-8244.
- [4] NÁDAŽDY, V., SCHAUER, F. and GMUCOVÁ, K. Energy resolved electrochemical impedance spectroscopy for electronic structure mapping in

- organic semiconductors. *Applied Physics Letters*. 2014, vol. 105, no. 14, p. 142109. ISSN 0003-6951.
- [5] MAYER, H. C. and KRECHETNIKOV, R. Landau-Levich flow visualization: Revealing the flow topology responsible for the film thickening phenomena. *Physics of Fluids* [online]. 2012, vol. 24, no. 5, p. 052103. ISSN 1070-6631.
- [6] KREBS, F. C. Fabrication and processing of polymer solar cells: A review of printing and coating techniques. *Solar Energy Materials and Solar Cells* [online]. 2009, vol. 93, no. 4, p. 394-412. ISSN 0927-0248.
- [7] YONKOSKI, R. K. and SOANE, D. S. Model for Spin Coating in Microelectronic Applications. *Journal of Applied Physics* [online]. 1992, vol. 72, no. 2, p. 725-740. ISSN 0021-8979.
- [8] WASHO, B. D. Rheology and Modeling of the Spin Coating Process. *IBM Journal of Research and Development* [online]. 1977, vol. 21, no. 2, p. 190-198. ISSN 0018-8646.
- [9] URBÁNEK, P., KUŘITKA, I., DANIŠ, S., TOUŠKOVÁ, J. and TOUŠEK, J. Thickness threshold of structural ordering in thin MEH-PPV films. *Polymer*. 2014, vol. 55, no. 16, p. 4050-4056. ISSN 0032-3861.
- [10] HÖFLE, S., LUTZ, T., EGEL, A., NICKEL, F., KETTLITZ, S. W., GOMARD, G., LEMMER, U. and COLSMANN, A. Influence of the Emission Layer Thickness on the Optoelectronic Properties of Solution Processed Organic Light-Emitting Diodes. *ACS Photonics* [online]. 2014, vol. 1, no. 10, p. 968-973. ISSN 2330-4022.
- [11] SKODA, D., URBANEK, P., SEVCIK, J., MUNSTER, L., NADAZDY, V., CULLEN, D. A., BAZANT, P., ANTOS, J. and KURITKA, I. Colloidal cobalt-doped ZnO nanoparticles by microwave-assisted synthesis and their utilization in thin composite layers with MEH-PPV as an electroluminescent material for polymer light emitting diodes. *Organic Electronics* [online]. 2018, vol. 59, p. 337-348. ISSN 1566-1199.
- [12] SKODA, D., URBANEK, P., SEVCIK, J., MUNSTER, L., ANTOS, J. and KURITKA, I. Microwave-assisted synthesis of colloidal ZnO nanocrystals and their utilization in improving polymer light emitting diodes efficiency. *Materials Science and Engineering B-Advanced Functional Solid-State Materials* [online]. 2018, vol. 232, p. 22-32. ISSN 0921-5107.
- [13] JAMATIA, T., SKODA, D., URBANEK, P., SEVCIK, J., MASLIK, J., MUNSTER, L., KALINA, L. and KURITKA, I. Microwave-assisted synthesis of  $\text{FexZn1-xO}$  nanoparticles for use in MEH-PPV nanocomposites and their application in polymer light-emitting diodes. *Journal of Materials Science: Materials in Electronics* [online]. 2019. ISSN 1573-482X. Available on: <https://doi.org/10.1007/s10854-019-01473-z>.

- [14] ALAM, M. M. and JENEKHE, S. A. Polybenzobisazoles are efficient electron transport materials for improving the performance and stability of polymer light-emitting diodes. *Chemistry of Materials* [online]. 2002, vol. 14, no. 11, p. 4775-4780. ISSN 0897-4756.
- [15] UDHIARTO, Arief, HARYANTO, L. M., KHOERUN, B. and HARTANTO, D. *Effect of Anode and Cathode Workfunction on the Operating Voltage and Luminance of a Single Emissive Layer Organic Light Emitting Diode* [online]. , 2017. + p. ISBN 978-1-5090-6397-0. PT: B; CT: 15th International Conference on Quality in Research (QiR) - International Symposium on Electrical and Computer Engineering; CY: JUL 24-27, 2017; CL: Bali, INDONESIA; SP: Univ Indonesia, Facul Eng, Univ Udayana Fakultas Teknik, Politeknik Negeri Bali, Starborn PT luas Birus Utama, Pertamina Aviat, Queensland Univ Techonol, Waskita, Bank Bukopin; UT: WOS:000426990300013.
- [16] HSIAO, C., HSIAO, A. and CHEN, S. Design of hole blocking layer with electron transport channels for high performance polymer light-emitting diode. *Advanced Materials* [online]. 2008, vol. 20, no. 10, p. 198-+. ISSN 0935-9648.
- [17] HSIAO, C. C., CHANG, C. H., JEN, T. H., HUNG, M. C. and CHEN, S. A. High-efficiency polymer light-emitting diodes based on poly[2-methoxy-5-(2-ethylhexyloxy)-1,4-phenylene vinylene] with plasma-polymerized CHF<sub>3</sub>-modified indium tin oxide as an anode. *Applied Physics Letters* [online]. 2006, vol. 88, no. 3, p. 033512. ISSN 0003-6951.
- [18] TSENG, S., LI, S., MENG, H., YU, Y., YANG, C., LIAO, H., HORNG, S. and HSU, C. High-efficiency blue multilayer polymer light-emitting diode based on poly(9,9-dioctylfluorene). *Journal of Applied Physics* [online]. 2007, vol. 101, no. 8, p. 084510. ISSN 0021-8979.
- [19] HUANG, Q., ZHAO, S., GUO, L. J., XU, Z., WANG, P. and QIN, Z. Effect of the charge balance on high-efficiency inverted polymer light-emitting diodes. *Organic Electronics* [online]. 2017, vol. 49, p. 123-128. ISSN 1566-1199.
- [20] YIN, X., XIE, G., PENG, Y., WANG, B., CHEN, T., LI, S., ZHANG, W., WANG, L. and YANG, C. Self-Doping Cathode Interfacial Material Simultaneously Enabling High Electron Mobility and Powerful Work Function Tunability for High-Efficiency All-Solution-Processed Polymer Light-Emitting Diodes. *Advanced Functional Materials* [online]. 2017, vol. 27, no. 26, p. 1700695. ISSN 1616-301X.
- [21] ZHENG, H., ZHENG, Y., LIU, N., AI, N., WANG, Q., WU, S., ZHOU, J., HU, D., YU, S., HAN, S., XU, W., LUO, C., MENG, Y., JIANG, Z., CHEN, Y., LI, D., HUANG, F., WANG, J., PENG, J. and CAO, Y. All-solution processed polymer light-emitting diode displays. *Nature Communications* [online]. 2013, vol. 4, p. 1971. ISSN 2041-1723.

- [22] PARK, B., BAE, I., NA, S. Y., AGGARWAL, Y. and HUH, A. Y. H. High brightness and efficiency of polymer-blend based light-emitting layers without the assistance of the charge-trapping effect. *Optics Express* [online]. 2019, vol. 27, no. 12, p. A693-A706. ISSN 1094-4087.
- [23] SYUE, H., HUNG, M., CHANG, Y., LIN, G., LEE, Y. and CHEN, S. High Brightness Fluorescent White Polymer Light-Emitting Diodes by Promoted Hole Injection via Reduced Barrier by Interfacial Dipole Imparted from Chlorinated Indium Tin Oxide to the Hole Injection Layer PEDOT:PSS. *Acs Applied Materials & Interfaces* [online]. 2017, vol. 9, no. 4, p. 3824-3830. ISSN 1944-8244.
- [24] FARIA, J. C. D., CAMPBELL, A. J. and MCLACHLAN, M. A. ZnO Nanorod Arrays as Electron Injection Layers for Efficient Organic Light Emitting Diodes. *Advanced Functional Materials* [online]. 2015, vol. 25, no. 29, p. 4657-4663. ISSN 1616-301X.
- [25] DAVIDSON-HALL, T. and AZIZ, H. The role of polyethylenimine in enhancing the efficiency of quantum dot light-emitting devices. *Nanoscale* [online]. 2018, vol. 10, no. 5, p. 2623-2631. ISSN 2040-3364.
- [26] CHOI, M. K., YANG, J., KIM, D. C., DAI, Z., KIM, J., SEUNG, H., KALE, V. S., SUNG, S. J., PARK, C. R., LU, N., HYEON, T. and KIM, D. Extremely Vivid, Highly Transparent, and Ultrathin Quantum Dot Light-Emitting Diodes. *Advanced Materials* [online]. 2018, vol. 30, no. 1, p. 1703279. ISSN 0935-9648.
- [27] CAO, W., XIANG, C., YANG, Y., CHEN, Q., CHEN, L., YAN, X. and QIAN, L. Highly stable QLEDs with improved hole injection via quantum dot structure tailoring. *Nature Communications* [online]. 2018, vol. 9, p. 2608. ISSN 2041-1723.
- [28] SERNELIUS, B. E., BERGGREN, K. F., JIN, Z. C., HAMBERG, I. and GRANQVIST, C. G. Band-Gap Tailoring of ZnO by Means of Heavy Al Doping. *Physical Review B* [online]. 1988, vol. 37, no. 17, p. 10244-10248. ISSN 0163-1829.
- [29] MA, Z., LUO, C., WANG, C. and LIU, J. Study of optical properties of ZnO doped with Fe. *Optik* [online]. 2019, vol. 188, p. 104-109. ISSN 0030-4026.
- [30] WANG, Y. S., THOMAS, P. J. and O'BRIEN, P. Optical properties of ZnO nanocrystals doped with Cd, Mg, Mn, and Fe ions. *Journal of Physical Chemistry B* [online]. 2006, vol. 110, no. 43, p. 21412-21415. ISSN 1520-6106.
- [31] CHEN, S., SONG, R., WANG, J., ZHAO, Z., JIE, Z., ZHAO, Y., QUAN, B., HUANG, W. and LIU, S. Improved performances in top-emitting organic light-emitting diodes based on a semiconductor zinc oxide buffer

- layer. *Journal of Luminescence* [online]. 2008, vol. 128, no. 7, p. 1143-1147. ISSN 0022-2313.
- [32] LUO, Y., YU, T., NIAN, L., LIU, L., HUANG, F., XIE, Z. and MA, Y. Photoconductive Cathode Interlayer for Enhanced Electron Injection in Inverted Polymer Light-Emitting Diodes. *Acs Applied Materials & Interfaces* [online]. 2018, vol. 10, no. 13, p. 11377-11381. ISSN 1944-8244.
- [33] SKODA, D., URBANEK, P., SEVCIK, J., MUNSTER, L., ANTOS, J. and KURITKA, I. Microwave-assisted synthesis of colloidal ZnO nanocrystals and their utilization in improving polymer light emitting diodes efficiency. *Materials Science and Engineering B-Advanced Functional Solid-State Materials* [online]. 2018, vol. 232, p. 22-32. ISSN 0921-5107.

## LIST OF TABLES

Table 1 Highlighted diffusion lengths of excitons and their dependency on film thickness. The values without reference are newly obtained. ....	14
Table 2 Highlighted parameters of PLEDs with neat MEH-PPV as an active layer.....	17
Table 3 Highlighted parameters of PLEDs with ZnO nanoparticles incorporated in 150 nm thick active layer with MEH-PPV matrix .....	18
Table 4 Highlighted parameters of PLEDs with ZnO nanoparticles incorporated in 35 nm thick nanocomposite layer with MEH-PPV matrix.....	20
Table 5 Basic properties of Fe doped nanoparticles. ....	21
Table 6 Highlighted parameters of PLEDs with Fe: ZnO nanoparticles incorporated in 35 nm thick nanocomposite layer with MEH-PPV matrix. ....	22
Table 7 Basic properties of Al doped nanoparticles. ....	24
Table 8 Highlighted parameters of PLEDs with Al: ZnO nanoparticles incorporated in 35 nm thick nanocomposite layer with MEH-PPV matrix. ....	26
Table 9 Summary of performance of prepared PLEDs measured @ 10V. ....	27

## LIST OF FIGURES

Figure 1. The schematic representation of a simple OLED device structure .....	4
Figure 2 Sample arrangement of ER-EIS method.....	6
Figure 3 Scheme of fabrication of PLED; a) glass with patterned ITO, b) deposition of HTL PEDOT:PSS, c) Deposition of active layer; d) Sputtering of metal Cathode.....	11
Figure 4 A representative of the SPV measurement and evaluation of diffusion length of excitons. Own source.....	13
Figure 5 Emission scans of prepared thin nanocomposite films based on MEH-PPV conjugated polymer.....	15
Figure 6. The density of states of MEH-PPV MEH-PPV/ZnO and MEH-PPV/AlZnO layers with thickness approx. 100 nm .....	15
Figure 7 Intensity of electroluminescence of PLED devices MEH-PPV/commercial ZnO as an active layer with input voltage 10 V and 1 s integration time .....	18
Figure 8 TEM micrographs of ZnO nanoparticles prepared from solutions with various precursor concentration. The average size of particles is 4, 8, 11, and 14 nm for samples ZnO 1, 2, 3 and 4, respectively.....	19
Figure 9 Intensity of electroluminescence of PLED devices with different size of nano ZnO in the active layer, input voltage 10 V and 1s integration time.....	19
Figure 10 TEM images of $\text{Fe}_x\text{Zn}_{(1-x)}\text{O}$ nanoparticles .....	21
Figure 11 EL intensity of devices with Fe:ZnO at 10 V and 1s integration time.....	22
Figure 12 TEM images of $\text{Al}_x\text{Zn}_{(1-x)}\text{O}$ nanoparticles .....	23
Figure 13 I-V characteristic of PLEDs with $\text{Al}_x\text{Zn}_{(1-x)}\text{O}/\text{MEH-PPV}$ .....	25
Figure 14 EL intensity of devices with Al:ZnO at 10 V and 1s integration time.....	25
Figure 15 Comparison of band structure of prepared polymer and nanocomposite light-emitting devices. ....	29

## LIST OF ABBREVIATIONS AND ACRONYMS

AFM	Atomic-force microscopy
CP	Conjugated polymer
DOS	Density of states
ER-EIS	Energy-resolved Electrochemical impedance spectroscopy
ETL	Electron transporting layer
FF	Fill factor
HJ	Hetero-junction
HOMO	Highest occupied molecular orbital
HTL	Hole transporting layer
ITO	Indium tin oxide
I-V	Current voltage
LED	Light-emitting diode
LEP	Light emitting polymer
LUMO	Lowest unoccupied molecular orbital
MOSFET	Metal-oxide-semiconductor field-effect transistor
OFET	Organic field-effect transistors
OLED	Organic light-emitting diode
OPD	Organic photodetectors
OPV	Organic photovoltaic
OSC	Organic semiconductor
PL	Photoluminescence
PLED	Polymer light-emitting diode
SCR	Space-charge region
SEM	Scanning electron microscopy
SM-OLED	Small-molecule organic light-emitting diode
SPV	Surface photovoltage
TLC	Trap-limited current

## LIST OF SYMBOLS

$\Delta n(x)$	excess excitons concentration at depth x in bulk
$[A]$	concentration of redox pair in electrolyte
$2\theta_{1/2}$	apex angle
$A_{PLED}$	the active area of the prepared device
$c$	volume fraction of solids
$CE$	current efficiency
$d$	thickness of bulk
$DLE$	diffusion length of exciton
$E$	elemental charge
$E_{act}$	activation energy of the conductivity
$E_F$	fermi energy level
$E_T$	energetic depth of trap
$G$	factor represents recombination losses in the SCR
$g(x)$	photogeneration rate
$I$	discharge current
$I_0$	photon flux density
$I_{vX}$	luminous intensity, X stands for indices PLED, REF – reference diode, HS – hyphothetic source
$J, J_S$	current density
$J_B, J_S$	multiplied by $a_1$ represent the SPV signal generated by photons
$J_{SCL}$	space limited current
$J_{TLC}$	trap limited current
$k$	constant of proportionality
$K$	constant ( $81Q/16 \pi$ )
$K_B$	Boltzmann's constant
$K_{et}$	coefficient of charge-transfer
$L$	layer thickness
$L_{vX}$	luminance, X stands for indices PLED, REF – reference diode,
$N_C$	effective density of states in LUMO

$n_s$	electrons concentration on semiconductor surface
$N_T$	density of traps
$Q$	amount of sputtered material or volumetric flow rate
$q_{eff}$	radiation of exciton efficiency
$R$	disk radius or symmetrical dimension of the sample
$R_1, R_2$	reflectance from the illuminated and the bottom surfaces
$R_{CT}$	charge transfer resistance
$R_I$	ratio between the 0-0 peak area and the sum of 0-1 and 0-2
$s$	surface recombination velocity
$T_V$	evaporation temperature
$V$	applied, photogenerated or working voltage
$v_d$	mean of drift transport velocity
$w$	thickness of SCR (space-charge region)
$\alpha$	absorption coefficient
$\gamma$	equilibrium of charge carriers
$\delta$	dry coating thickness
$\varepsilon$	electric field intensity
$\varepsilon_0, \varepsilon_r$	dielectric constants
$\eta_{EQE}$	external quantum efficiency
$\eta_{out}$	number of radiative photons
$\eta_{ST}$	singlet/triplet excitons ratio
$\mu$	mobility of charge carriers
$\nu$	kinematic viscosity
$\sigma$	conductivity
$\sigma_0$	theoretical maximum of conductivity
$\Phi_X$	luminous flux, X stands for indices PLED, REF – reference diode,
$\omega$	frequency of alternative current or angular velocity
$\Omega$	three-dimensional angular span, solid angle

# CURRICULUM VITAE

## **Name and Surname**

Jakub Ševčík.

## **Personal information**

Male, born in Zlín, 4<sup>th</sup> July 1990.

Nationality: Czech

Address: Masarykova 994, 76326, Luhačovice, The Czech Republic

Telephone / Mobile: +420 777 852 613

E-mail: j4sevcik@utb.cz

## **Education**

Dates: 2015 – to date

Doctoral studies in Chemistry and Materials Technology, Specialization: Technology of Macromolecular Compounds; Faculty of Technology, Tomas Bata University in Zlín

Dates: 2013 - 2015

Title of qualification awarded: Ing.

Master's program in Chemistry and Materials Technology, degree course in Polymer engineering, specialization Medical and Pharmaceutical Materials; Faculty of Technology, Tomas Bata University in Zlín

Master's thesis topic: Preparation and characterisation of thin films applicable in organic electronics

Dates: 2011 - 2013

Title of qualification awarded: Bc.

Bachelor's program in Chemistry and Materials Technology, degree course in Polymer materials and technology, specialization Medical and Pharmaceutical Materials; Faculty of Technology, Tomas Bata University in Zlín

Bachelor's thesis topic: Preparation and characterisation of thin films

Dates: 2006 - 2010

J. A. Komenský Grammar School Valašské Klobouky

Completed with a school-leaving examination in: Czech language, German language, chemistry, biology

## LIST OF PROJECTS

1. IGA/CPS/2015/006 – Preparation of functional inks for material inkjet printing and their applications in printed electronics and sensors – member of the research team
2. IGA/CPS/2016/007 – Preparation and characterization of functional polymer materials for thin films applicable in printed electronics and sensor technology – project leader
3. IGA/CPS/2017/008 – Preparation and characterization of nanoparticles and thin nanocomposite films made thereof – member of the research team
4. IGA/CPS/2018/007 – Development and studies of conductive nanocomposite systems applicable in polymer electronics – member of the research team
5. IGA/CPS/2019/007 – Development and study of conductive nanocomposite materials for electronic and electrotechnical applications – member of the research team
6. NPU I LO1504 – Centre of Polymer Systems plus – research project worker
7. TE01020216 – The Technology Agency of the Czech Republic (TA CR) – research project worker
8. GA19-23513S - Towards New Electroluminescent Materials: Borane Cluster Compounds in Thin Polymer Films within an Electric Field – member of the research team

## LIST OF PUBLICATIONS

### *Journal papers:*

1. CVEK, Martin, Miroslav MRLIK, Jakub SEVCIK and Michal SEDLACIK. Tailoring Performance, Damping, and Surface Properties of Magnetorheological Elastomers via Particle-Grafting Technology. *Polymers* [online]. 2018, vol. 10, no. 12, s. 1411. ISSN 2073-4360.
2. JAMATIA, Thaiskang, David SKODA, Pavel URBANEK, Jakub SEVCIK, Jan MASLIK, Lukas MUNSTER, Lukas KALINA and Ivo KURITKA. Microwave-assisted synthesis of  $\text{FexZn}_{1-x}\text{O}$  nanoparticles for use in MEH-PPV nanocomposites and their application in polymer light-emitting diodes. *Journal of Materials Science: Materials in Electronics* [online]. 2019. ISSN 1573-482X. Dostupné z: <https://doi.org/10.1007/s10854-019-01473-z>.
3. SKODA, David, Pavel URBANEK, Jakub SEVCIK, Lukas MUNSTER, Vojtech NADAZDY, David A. CULLEN, Pavel BAZANT, Jan ANTOS and Ivo KURITKA. Colloidal cobalt-doped ZnO nanoparticles by microwave-assisted synthesis and their utilization in thin composite layers with MEH-

PPV as an electroluminescent material for polymer light emitting diodes. *Organic Electronics* [online]. 2018, vol. 59, s. 337-348. ISSN 1566-1199.

4. SKODA, David, Pavel URBANEK, Jakub SEVCIK, Lukas MUNSTER, Jan ANTOS and Ivo KURITKA. Microwave-assisted synthesis of colloidal ZnO nanocrystals and their utilization in improving polymer light emitting diodes efficiency. *Materials Science and Engineering B-Advanced Functional Solid-State Materials* [online]. 2018, vol. 232, s. 22-32. ISSN 0921-5107.
5. URBANEK, Pavel, Ivo KURITKA, Jakub SEVCIK, Jana TOUSKOVA, Jiri TOUSEK, Vojtech NADAZDY, Peter NADAZDY, Karol VEGSO, Peter SIFFALOVIC, Radka RUTSCH and Michal URBANEK. An experimental and theoretical study of the structural ordering of the PTB7 polymer at a mesoscopic scale. *Polymer* [online]. 2019, vol. 169, s. 243-254. ISSN 0032-3861.

### **Conferences:**

6. JAMATIA Thaiskang, Pavel URBANEK, Lukas MUNSTER, Jakub SEVCIK and Ivo KURITKA. *Tailoring of band gap and optical properties of ZnO nanoparticles by doping with Fe*. Frankfurt, Germany. November 06-08, 2017.
7. SEVCIK, Jakub, Pavel URBANEK, Pavol SULY, Michal URBANEK, Jan MASLIK, Jan ANTOS and Ivo KURITKA. *Preparation and Characterization of Nanostructured Thin Films Applicable in Polymer Light Emitting Devices* [online]., 2017. 821 s. ISBN 978-80-87294-71-0. PT: B; CT: 8th International Conference on Nanomaterials - Research and Application (NANOCON); CY: OCT 19-21, 2016; CL: Brno, CZECH REPUBLIC; SP: TANGER Ltd, Reg Ctr Adv Technologies & Mat, Czech Soc New Mat & Technologies; UT: WOS:000410656100142.
8. URBANEK, Michal, Michal MACHOVSKY, Pavel URBANEK, Jakub SEVCIK and Ivo KURITKA. *Cross Sectioning of Optoelectronic Device* [online]., 2017. 791 s. ISBN 978-80-87294-71-0. PT: B; CT: 8th International Conference on Nanomaterials - Research and Application (NANOCON); CY: OCT 19-21, 2016; CL: Brno, CZECH REPUBLIC; SP: TANGER Ltd, Reg Ctr Adv Technologies & Mat, Czech Soc New Mat & Technologies; UT: WOS:000410656100137.
9. JAMATIA, Thaiskang, Pavel URBANEK, David SKODA, Jakub SEVCIK and Ivo KURITKA. Microwave-assisted particle size-controlled synthesis of ZnO nanocolloids and its application in fabrication of PLED devices: Applied Nanotechnology and Nanoscience International Conference, Berlin, Germany 2018. (poster, full text contribution in proceedings journal issue) IOP Conf. Series: Journal of Physics: Conf. Series vol. 1310 (2019) 01201

## **OVERVIEW OF OTHER ACTIVITIES**

### ***Pedagogic activities:***

Participated on teaching in laboratory classes of “Preparation and Characterization Methods” and “Applicable Spectroscopy”.

### ***Trainings:***

Measurement of vibration spectra – University of Chemistry and Technology (Prague 2016)

Interpretation of vibration spectra – University of Chemistry and Technology (Prague 2016)

The Basics of Raman spectroscopy and Nano-objects microscopy (Prague 2017)

### ***Technical Internships:***

Internship at Charles University at the faculty of Mathematics and Physics at the department of Macromolecule Physics (Prague 2017) during 6/11 to 5/12 2017

Internship in Charles University at the faculty of Mathematics and Physics at the department of Macromolecule Physics (Prague 2017) during 14/1 to 25/1 2019

### ***International stay***

Erasmus+ stay at the Rzeszów University of Technology, Faculty of Chemistry Poland. 2 months – from 1<sup>st</sup> August 2019 to 30<sup>th</sup> September 2019.

Jakub Ševčík

**Příprava a charakterizace nanokompozitních tenkých filmů s  
využitím v organické elektronice**

Preparation and characterisation of nanocomposite thin films applicable in  
organic electronics

Doctoral Thesis Summary

Published by: Tomas Bata University in Zlín,  
nám. T. G. Masaryka 5555, 760 01 Zlín.

Edition: published electronically

Typesetting: Jakub Ševčík

This publication has not undergone any proofreading or editorial review.

Year of Publication 2019

First edition

ISBN 978-80-7454-890-1

